Coordination Chemistry Reviews 257 (2013) 3202–3221

Contents lists available at ScienceDirect

Coordination Chemistry Reviews

journal homepage: www.elsevier.com/locate/ccr

Review

Molecular precursor approach to metal oxide and pnictide thin films

Peter Marchand, Claire J. Carmalt*

Department of Chemistry, University College London, Christopher Ingold Laboratories, 20 Gordon St., London WC1H 0AJ, UK

Contents

1. Introduction 3202
2. Precursors to gallium and indium oxide 3203
   2.1. Donor-functionalized alkoxides 3204
   2.2. Multidentate alkoxides 3208
   2.3. Sesquialkoxides 3208
   2.4. β-Diketonates and β-ketoiminates 3209
   2.5. Gallium-doped indium oxide 3212
   2.6. Combinatorial CVD of gallium indium oxide 3213
   2.7. Transition metal-doped indium oxide 3214
3. Precursors to bismuth oxide 3214
   3.1. Alkoxides and β-diketonates 3214
4. Precursors to transition metal pnictides 3215
   4.1. Titanium and zirconium guanidinates 3216
   4.2. Transition metal imido complexes 3216
   4.3. Titanium phosphine and arsine complexes 3218
5. Conclusion 3219
   Acknowledgements 3220
   References 3220

ARTICLE INFO

Article history:
Received 30 November 2012
Received in revised form 24 January 2013
Accepted 24 January 2013
Available online 18 February 2013

Keywords:
Gallium oxide
Indium oxide
Single-source precursors
Bismuth oxide
Titanium nitride
Tungsten nitride
Titanium phosphide
Titanium arsenide
Zirconium carbonitride
Chemical vapour deposition

ABSTRACT

Molecular precursors for the preparation of main group metal oxide and transition metal pnictide thin films have been developed. This work involves the design and synthesis of single-source precursors that contain all the elements required in the thin film. Design of the ideal precursor presents a significant challenge since they must be volatile, non-toxic and thermally stable. Therefore the precursors have been tailored to give clean, reproducible decomposition leading to high quality thin films with good coverage of the substrate. In this review key aspects of precursor synthesis and thin film deposition developed in our group are described. The range of precursors developed for main group oxides, in particular gallium and indium oxide, are discussed, with the most studied being the donor-functionalized alkoxides of the type $[R_2M(OR')]_2$ (M = Ga, In; R = H, Me, Et; R′ = $CH_2CH_2NMe_2$, CH_2CH_2OMe etc.). Preliminary mechanistic studies suggest that monomers are formed in the gas phase via stabilization of the metal centre by the donor atom (N or O). Precursors to transition metal pnictides have also been developed, including guanidinates, imides, phosphine and arsine compounds and an overview of their use in film deposition is given.

1. Introduction

The most common approach for the chemical vapour deposition (CVD) of many materials, such as oxides, nitrides, phosphides and arsenides, is to use two or more separate precursors that react individually on the growing film [1]. This procedure, however, makes it difficult to control film stoichiometry and usually high

* Corresponding author. Tel.: +44 2076797528.
E-mail address: c.j.carmalt@ucl.ac.uk (C.J. Carmalt).

0010-8545
http://dx.doi.org/10.1016/j.ccr.2013.01.030

deposition temperatures are required. In addition, in some cases, toxic or pyrophoric materials are utilized in the production of the films. Another approach to such materials is to use a single-source precursor, which consists of the elements (M—E) in the material (e.g. M = Ga and E = O for Ga_2O_3) bonded at the core of the molecule, with various other ligands attached to each of the elements [2]. The reaction pathway involves adsorption of the precursor without breaking the M—E bond but with loss of the ancillary ligands, affording a thin film of the desired material. The advantages of the single-source precursor approach are fourfold. First, the stoichiometry of the precursor can be retained in the film. Second, the high deposition temperatures often associated with multi-source depositions are generally lowered. Third, the precursor delivery system can be simplified. Fourth, better homogeneity is possible since the desired elements are effectively premixed at the molecular level. Thus, single-source precursors can provide a simple and clean route to films, eliminating the need for a mixture of precursors which can often be toxic and/or expensive, as well as involving complicated gas-phase reaction dynamics which can result in the formation of non-stoichiometric films [2,3].

Despite the numerous advantages outlined above, there are disadvantages to using single-source precursors, for example, such precursors often have low vapour pressures, contamination of the films can result from the decomposition of the ligand and the stoichiometry of the precursor is not always retained in the film. However, advances in variants of deposition techniques, such as CVD, have gone some way to overcome many of these issues. For example, aerosol-assisted (AA)CVD, a variant of conventional CVD processes, addresses the delivery and availability problems associated with single-source precursors [4,5]. AACVD uses a liquid–gas aerosol to transport soluble precursors to a heated substrate and is a useful method when a conventional atmospheric or low pressure CVD precursor proves involatile or thermally unstable. Compared to conventional CVD, the AACVD method uses aerosol droplets to transport precursors, with the aid of inert carrier gases. Therefore, in AACVD volatility is no longer crucial and this allows for a wider choice of precursors being available for use and can lead to high quality films at low cost. AACVD can also result in high deposition rates due to the possibility of high mass-transport rate of the precursor, as well as simplification of the delivery. By designing precursors specifically for AACVD, the restrictions of volatility and thermal stability are lifted, and new precursors and films can be investigated. Furthermore, different and unique morphologies of films can be obtained by AACVD due to the influence of the solvent on the deposition, which could potentially lead to improved properties.

Our main efforts have concentrated on the preparation of precursors and their subsequent deposition to thin films of metal oxides and nitrides although this has been extended to other materials. Recent research has concentrated on the synthesis of precursors for the production of gallium and indium oxide thin films using AACVD, as well as combinatorial AACVD (cAACVD). A variety of methods to deposit these films exists, as do a large selection of well-defined molecular compounds which contain a preformed M—O bond (M = Ga, In) that can be used in deposition processes without an additional oxygen input, i.e. single-source precursors. However, we have developed a range of precursors for main group oxides, with the most studied being the donor-functionalized alkoxides, of the type $[R_2M(OR')]_2$ (M = Ga, In; R = H, Me, Et; R′ = $CH_2CH_2NMe_2$, CH_2CH_2OMe etc.). These ligands were chosen for AACVD as they lead to precursors which are less air/moisture sensitive and have increased solubility. The high moisture sensitivity of many main group alkoxides makes them difficult to use in solution-based CVD [6]. Therefore, modified alkoxides, such as the donor functionalized ligands, which have an increased coordinative saturation at the metal centre, provide more stability and also eliminate the necessity of introducing an extra donor group to stabilize the electron deficient main group alkoxide complex. Moreover, preliminary mechanistic studies using gas phase electron diffraction indicates that monomers are formed in the gas phase via stabilization of the metal centre by the donor atom. Other ligand types that we have investigated include β-ketonates, β-ketoiminates and sesquialkoxides.

Another focus of our research has included precursors to transition metal pnictides – nitrides, phosphides and arsenides. The design, synthesis and use of transition metal guanidinates, imido, phosphine and arsine compounds as precursors to metal pnictide or metal carbonitride thin films has been investigated and some of the compounds have been shown to be good precursors for use in low pressure CVD. This review provides an overview of the deposition of main group oxide and transition metal pnictide thin films using the molecular precursors developed in our group. The following abbreviations will be used: acac (acetylacetonate); ALD (atomic layer deposition); bdk (β-diketonate); CVD (chemical vapour deposition); EDXA (energy dispersive X-ray analysis); GED (gas-phase electron diffraction), hfac (1,1,1,5,5,5-hexafluoroacetylacetonate); ITO (tin-doped indium oxide); py (pyridine); TCO (transparent conducting oxide), TGA (thermogravimetric analysis); thd (2,2,6,6-tetramethylheptane-3,5-dionate); TMEDA (*N*,*N*,*N*′,*N*′-tetramethylethylenediamine); SEM (scanning electron microscopy), XRD (X-ray diffraction), XPS (X-ray photoelectron spectroscopy), WDX (wavelength dispersive X-ray analysis).

2. Precursors to gallium and indium oxide

Gallium oxide (Ga_2O_3) and indium oxide (In_2O_3) thin films are of interest due to their range of applications, which are related to their particular properties [7]. Since In_2O_3 films are conductive and transparent to visible light, they are used as a transparent conducting oxide (TCO), particularly when doped with other elements. For example, tin-doped indium oxide (ITO) thin films, with typical conductivities of $(1–5) \times 10^3$ S/cm and optical transparencies of 85–90%, are employed on a massive scale in numerous optoelectronic device applications [8,9]. Other elements have also been incorporated into indium oxide to increase its conductivity, including fluorine [10], sulfur [11] and gallium [12]. Gallium has also been used to dope zinc oxide, producing transparent conductive films as an alternative to ITO thin films for optoelectronic and electronic devices such as flat panel displays [13], solar cells [14] and light-emitting diodes [15,16].

Ga_2O_3 films, in contrast, are semiconducting above 500 °C and can act as a gas sensor for reducing gases, such as CO and ethanol [17,18]. However, when using gallium oxide films above 900 °C, the concentration of oxygen present in a system can be detected and so the function of the gas sensor could be switched from reducing gases to oxidizing gases [19,20]. Indium oxide films have also been shown to act as effective sensors, for example In_2O_3-modified gallium oxide thin films have been reported to be sensitive to ozone concentration and Ta-doped In_2O_3 showed a selective response to ethanol [21,22]. Furthermore, In_2O_3 nanorods have been reported to have sensing properties to formaldehyde [23].

Further applications include the use of gallium oxide films in zeolite catalytic systems [24], as white-light-emitting luminophores [25,26] and as solid electrolytes (for example doped-$LaGaO_3$) [27]. In addition, nitrogen-doped In_2O_3 thin films have been reported as visible light photocatalysts where on doping with nitrogen, the band gap of In_2O_3 was reduced from 3.5 eV to approximately 2.0 eV, thus electromagnetic radiation in the visible region can split water [28]. Zinc-doped gallium oxide has also been

found to be an active photovoltaic device upon exposure to UV light [29].

All of the above applications have resulted in an increased research effort into both precursor design and deposition of these materials. A recent review (2011) comprehensively described the range of single-source precursors to gallium and indium oxide and the methods employed to deposit gallium and indium oxide thin films using these compounds. Potential precursors to these materials were also described [2] and readers are directed to this review for a full account of research in this area. In this section, we describe our contribution to the development of molecular precursors to these materials, with particular emphasis on precursor design, as well as a description of the films deposited and their functional properties. This section has been organized into 7 areas comprising (i) donor-functionalized alkoxides, (ii) multidentate alkoxides, (iii) sesquialkoxides, (iv) β-diketonates and β-ketoiminates, (v) gallium-doped indium oxide, (vi) combinatorial CVD of gallium-indium-oxide and (vii) transition metal-doped indium oxide.

2.1. Donor-functionalized alkoxides

Gallium and indium alkoxides are often used as molecular precursors to thin films of gallium and indium oxide [2]. However, the alkoxides of gallium and indium are typically dimeric/tetrameric due to the electron deficient nature of these elements [6]. It is generally accepted that monomeric compounds are preferable for CVD due to their assumed higher volatility when compared to dimeric or tetrameric equivalents. The addition of a Lewis base (e.g. NMe_3) or increasing the steric bulk of the alkoxides can yield monomeric derivatives although this increases the molecular weight of the compound and can reduce the volatility. An alternative method is to modify the alkoxide by forming a donor-functionalized alkoxide via attachment of a Lewis base to the ligand (e.g. $OCH_2CH_2NMe_2$) [30,31]. The tendency for gallium and indium alkoxide complexes to oligomerize can then be reduced by coordinatively saturating the metal centre with the extra Lewis base, and hence resulting in precursors with increased volatility.

Group 13 monoalkoxometallanes, of the type $[R_2M(OR')]_2$, incorporating donor-functionalized alcohols, were synthesized from the reaction of MR_3 with R′OH (M = Ga, R = Me, R′ = $C(CH_3)_2CH_2OMe$ **1** [32]; M = Ga, R = Et, R′ = $CH_2CH_2NMe_2$ **2**, $CH(CH_3)CH_2NMe_2$ **3**, $C(CH_3)_2CH_2OMe$ **4**, CH_2CH_2OMe **5**, $CH(CH_2NMe_2)_2$ **6** [33,34]; M = In, R = Me, R′ = $CH_2CH_2NMe_2$ **7**, $CH(CH_3)CH_2OMe$ **8**, $C(CH_3)_2CH_2OMe$ **9**, $CH(CH_3)CH_2NMe_2$ **10**, $CH(CH_2NMe_2)_2$ **11** [32,35]), according to Scheme 1.

The compounds were isolated as oxygen-bridged dimers in the solid state, which was confirmed crystallographically for complexes **1**–**4**, **6** and **7**–**11** (see for example Figs. 1 and 2). Typically, the centrosymmetric, four-membered M_2O_2 ring in the dimeric compounds is planar and each group 13 atom adopts a distorted trigonal bipyramidal geometry with the two alkyl groups in equatorial positions. The bridging alkoxide groups are located in both axial and equatorial positions, while the donor atom (N or O) of the alkoxide ligand is in the axial position.

Low pressure (LP)CVD of compounds **2**, **3** and **6** was investigated and these compounds were selected on the basis of thermogravimetric analysis (TGA) under N_2, which showed that they gave the best decomposition characteristics [33,34]. Light grey films on glass and quartz substrates were deposited from these precursors at 600 °C. Analysis of the films via a range of techniques (XRD, XPS, EDXA, SEM, UV–Vis) indicated that amorphous, oxygen-deficient films of gallium oxide had been deposited with band gaps of the films calculated to be ~4.3 eV, comparable to literature values for Ga_2O_3 of 4.2–4.9 eV [36]. The formation of amorphous films was expected for the deposition of gallium oxide at temperatures below 750 °C [37].

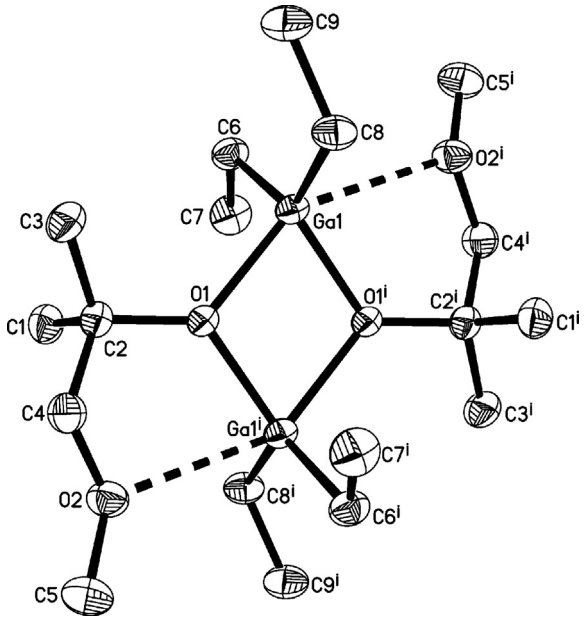

Fig. 1. X-ray structure of compound **4** with thermal ellipsoids shown at the 50% probability level (hydrogen atoms omitted for clarity).
Reprinted with permission from Ref. [33]. Copyright 2008 Elsevier.

The films grown via low pressure CVD were oxygen deficient probably due to the low oxygen content in the precursor. Therefore, AACVD reactions of MR_3 and excess donor-functionalized alcohol, R′OH, was investigated in an attempt to deposit higher purity gallium oxide and also indium oxide films since the presence of excess alcohol should reduce the oxygen deficiency of the films. These reactions between MR_3 and excess R′OH in toluene were assumed to generate in situ the group 13 monoalkoxometallanes, $[R_2M(OR')]_2$ (vide supra). The in situ reaction represents a rapid convenient route to the metal oxide films and eliminates the need for the synthesis, isolation and purification of single-source gallium and indium alkoxide precursor.

Amorphous Ga_2O_3 films were obtained from the AACVD reaction of GaR_3 and excess R′OH (R = Me, R′ = $C(CH_3)_2CH_2OMe$,

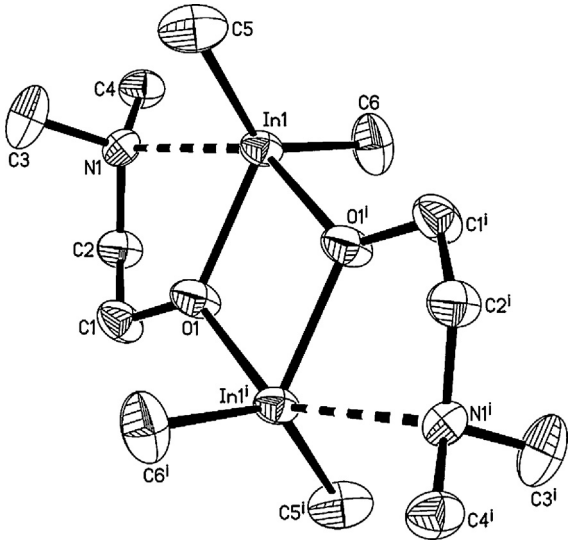

Fig. 2. X-ray structure of compound **7** with thermal ellipsoids shown at the 50% probability level (hydrogen atoms omitted for clarity).
Reprinted with permission from Ref. [35]. Copyright 2007 American Chemical Society.

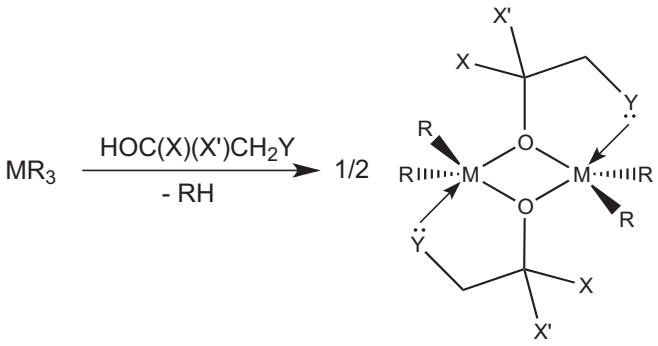

(**1**) M = Ga, R = Me, X = X' = CH_3, Y = OMe
(**2**) M = Ga, R = Et, X = X' = H, Y = NMe_2
(**3**) M = Ga, R = Et, X = CH_3, X' = H, Y = NMe_2
(**4**) M = Ga, R = Et, X = X' = CH_3, Y = OMe
(**5**) M = Ga, R = Et, X = X' = H, Y = OMe
(**6**) M = Ga, R = Et, X = CH_2NMe_2, X' = H, Y = NMe_2
(**7**) M = In, R = Me, X = X' = H, Y = NMe_2
(**8**) M = In, R = Me, X = CH_3, X' = H, Y = OMe
(**9**) M = In, R = Me, X = X' = CH_3, Y = OMe
(**10**) M = In, R = Me, X = CH_3, X' = H, Y = NMe_2
(**11**) M = In, R = Me, X = CH_2NMe_2, X' = H, Y = NMe_2

Scheme 1. Synthesis of compounds **1**–**11** [32–35].

CH_2CH_2OMe, $CH_2CH_2NMe_2$ [32]; M = Ga, R = Et, R′ = $CH_2CH_2NMe_2$, $CH(CH_3)CH_2NMe_2$, $C(CH_3)_2CH_2OMe$, $CH(CH_2NMe_2)_2$ [33]), which were superior to those deposited by LPCVD. Thus, the use of excess alcohol led to stoichiometric Ga_2O_3 films with low levels of carbon contamination (as determined by XPS). WDX showed the films to have a gallium to oxygen ratio close to the expected 1:1.5 for Ga_2O_3. The gallium oxide films displayed minimal reflectivity (5–10%) and high transmission (80–90%) and the band gap was calculated to range from 4.5 to 4.7 eV. SEM showed that the film morphology comprised of particles of size 100 nm in diameter but annealing the films in air at 600 °C resulted in a different morphology, with typical particle sizes of 1 μm and rods of about 10 μm (Fig. 3).

Films deposited using $GaMe_3$ were brown in contrast to transparent films grown when $GaEt_3$ was used as the gallium precursor, suggesting more incorporation of carbon in the former. The mechanism for the deposition process was not investigated. However, it is assumed to proceed via decomposition processes reported previously for related systems and the less carbon observed when using the ethyl-derivative is most likely due to a facile β-hydride elimination being available for this ligand (but not methyl). Thus, the ethyl (where appropriate) and R′ group from $[R_2Ga(OR')]_2$ were probably eliminated via β-hydride elimination when these complexes are pyrolyzed on or near the surface. The result of this would be the formation of intramolecular Ga—O bonds leading eventually to growth of Ga_2O_3.

AACVD of $InMe_3$ and excess R′OH (R′ = $CH_2CH_2NMe_2$, $C(CH_3)_2CH_2OMe$, $CH(CH_3)CH_2NMe_2$, CH_2CH_2OMe [32,35]) produced thin films of cubic crystalline In_2O_3, as shown by XRD patterns where strong reflections from the (2 2 2) plane were observed. Raman, XPS and WDX all provided further evidence for the formation of In_2O_3 (In:O ratio ~1:1.5) and conducting a Tauc plot [38] of the UV/visible data indicated that the films had band gaps ranging from 3.5 to 3.7 eV, in agreement with values previously reported (3.75 eV) [39]. Unusual film morphology can be obtained by AACVD due to the influence of the solvent on the deposition and the film morphology of the In_2O_3 films were studied using SEM. In most cases a needle-like morphology (needles ~4–10 μm in length) was apparent which is characteristic of an island growth mechanism (Fig. 4). However, the SEM of the films deposited from $InMe_3$ and $HOCH(CH_3)CH_2NMe_2$ suggests the formation of both spherical particles and needles, which could be due to the thickness of the film or the presence of both amorphous and crystalline material; all analysis indicated the deposition of only In_2O_3. In contrast, the SEM image for the film deposited from the reaction of $InMe_3$ and $HOCH_2CH_2NMe_2$ showed a different morphology, that of spherical particles. Since the same solvent (toluene) was used in all depositions, it possible that changing the R′ group on the alcohol could result in a change in morphology. The films were between 0.4 and 0.8 μm thick, determined using cross-sectional SEM.

Although we have used many of the compounds of the type $[R_2M(OR')]_2$ as precursors either in a LPCVD or AACVD process, little information is available on the gas-phase structures of such compounds or precursors in general employed for film growth. An understanding of the structures and behaviour of CVD precursors in the gas phase could potentially lead to improvements in precursor design and film growth and would provide important information about the decomposition processes central to

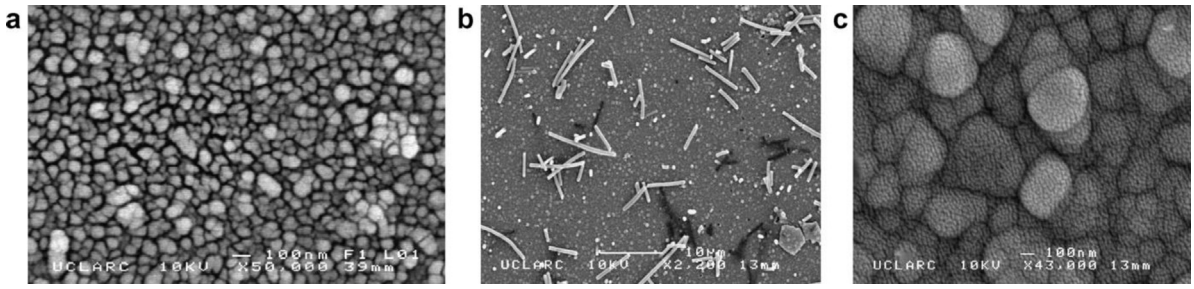

Fig. 3. SEM images for gallium oxide films deposited from the AACVD reaction of $GaEt_3$ and (a) $HOCH_2CH_2NMe_2$, (b) $HOCH_2CH_2NMe_2$ (post-annealing) and (c) $HOCH(CH_2NMe_2)_2$ at 450 °C.
Reprinted with permission from Ref. [33]. Copyright 2008 Elsevier Ltd.

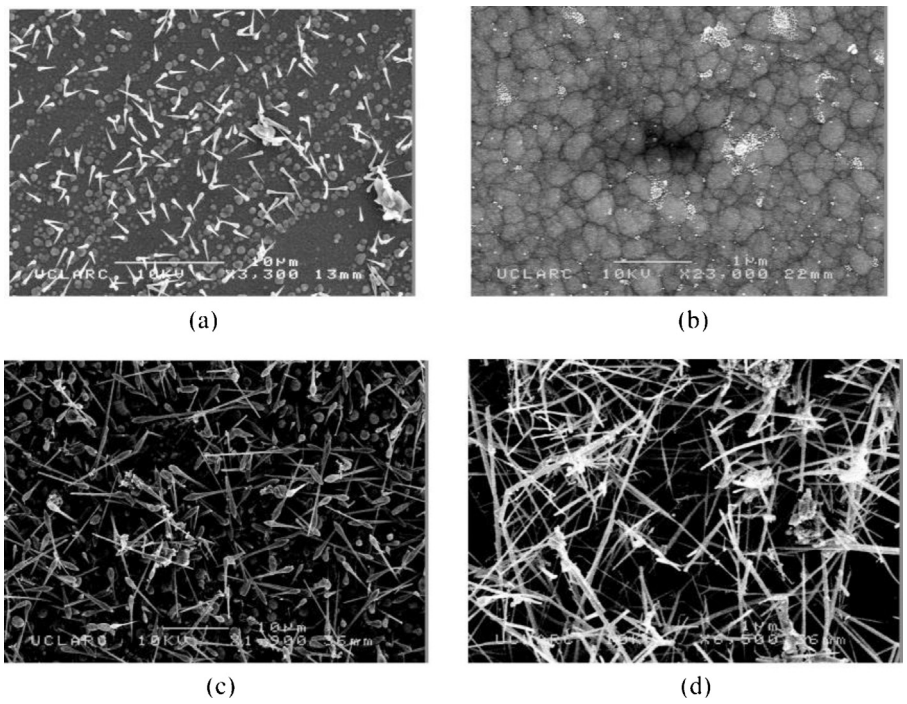

Fig. 4. SEM images for In_2O_3 films deposited from the reaction of $InMe_3$ and (a) $HOCH(CH_3)CH_2NMe_2$, (b) $HOCH_2CH_2NMe_2$, (c) $HOC(CH_3)_2CH_2OMe$, and (d) $HOCH_2CH_2OMe$ at 550 °C.
Reprinted with permission from Ref. [35]. Copyright 2007 American Chemical Society.

CVD [40]. We therefore determined the molecular structures of the vapours produced on heating dimethylalkoxygallanes, of the type $[Me_2Ga(OR')]_2$, by gas electron diffraction (GED) and ab initio molecular orbital calculations [41,42]. Three compounds were investigated, including $[Me_2Ga(OCH_2CH_2NMe_2)]_2$ (**12**) and $[Me_2Ga(OCH_2CH_2OMe)]_2$ (**13**) incorporating donor-functionalized alkoxides and for comparison the monofunctional alkoxide $[Me_2Ga(O^tBu)]_2$ (**14**) (Scheme 2). In the solid state **12**–**14** adopt dimeric structures with planar Ga_2O_2 rings, as described above, and these structures are retained in solution as shown by mass spectroscopy performed in toluene solution and ^1H NMR. Ab initio molecular orbital calculations

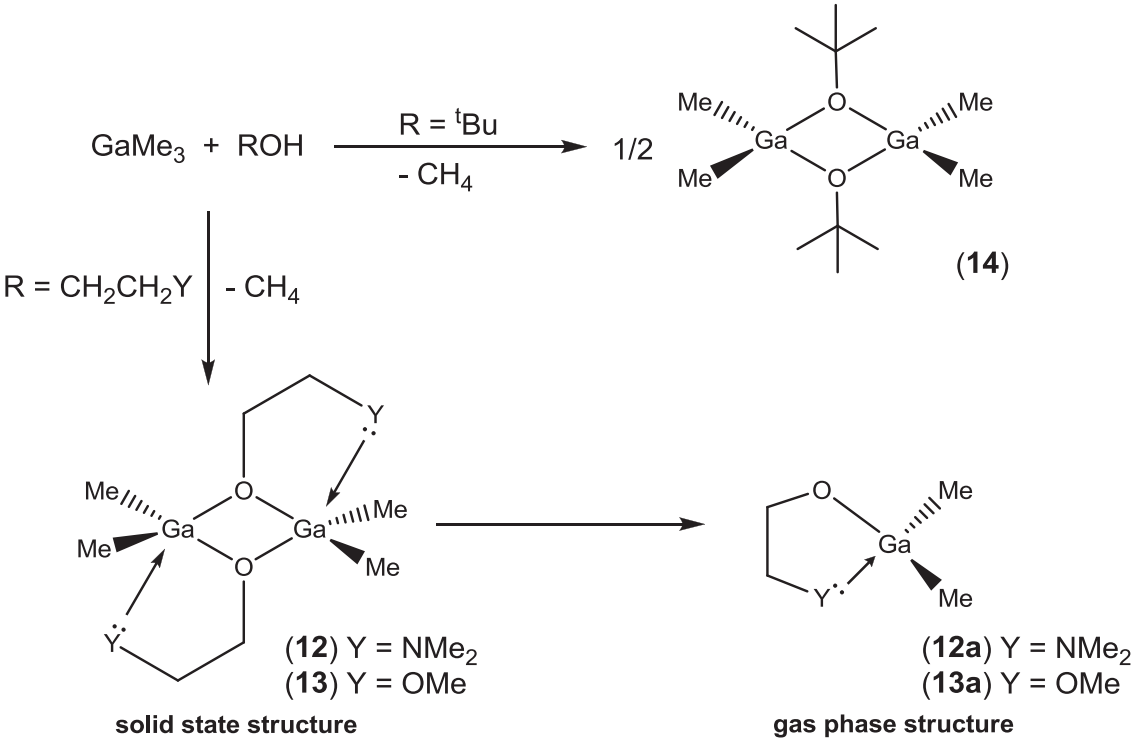

Scheme 2. Synthesis and solid-state and gas-phase structures of **12**–**14** [41].

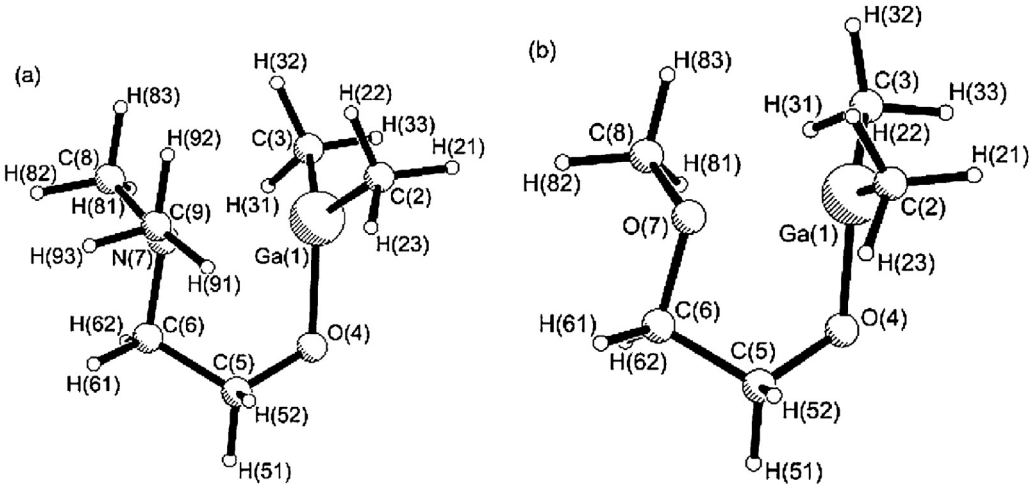

Fig. 5. Molecular structures of the monomeric species (a) compound **12a**, (b) compound **13a**, including atom numbering.
Reprinted with permission from Ref. [41]. Copyright 2012 American Chemical Society.

were performed for both the monomeric and dimeric forms of $[Me_2Ga(OCH_2CH_2NMe_2)]_n$ (**12a**, $n=1$; **12**, $n=2$) and $[Me_2Ga(OCH_2CH_2OMe)]_n$ (**13a**, $n=1$; **13**, $n=2$) since it was unclear whether the complexes would be monomeric, dimeric or both in the gas phase. Calculations for the dimers **12** and **13** indicated that in isolation they would have structures similar to those in the solid state. For each of the monomer structures, **12a** and **13a**, the possibility of closed-ring structures as well as open-chain conformers was considered and only one structure representing a minimum on the potential-energy surface was identified (C_1 symmetry), in which the gallium and donor atoms (nitrogen for **12a** and oxygen for **13a**) come close together to form a five-membered ring through dative bonding.

The structures of the vapours produced on heating **12**–**14** were studied by GED. For **12** and **13** the structures derived from the GED data were initially compared with theoretical data representing both dimeric and monomeric species. The fits to the monomers were far superior than those to the dimers and thus, only the monomeric forms **12a** and **13a**, were observed in the gas phase (Fig. 5). In contrast to **12** and **13**, compound **14** was found to be dimeric in the gas phase, as well as in the solid state. The gas-phase structures of **12a** and **13a** exhibit five-membered rings formed by a dative bond between Ga and the donor atom (N or O) from the donor-functionalized alkoxide. In **14** there is no possibility of a monomeric structure being stabilized by the formation of such a dative bond since only a monofunctional alkoxide is present in the molecule.

This difference in behaviour gives us an insight into the driving force behind the transition from dimer to monomer for **12** and **13**, potentially a key step in the decomposition process during CVD. Thus, although dialkylalkoxygallanes incorporating donor functionalized ligands generally adopt dimeric structures in the solid state, in the gas phase monomers are likely to be present. Monomers are expected to exhibit enhanced volatility in comparison to oligomeric complexes, in which intermolecular solid-state interactions are likely to increase the enthalpy of vaporization. However, this work shows that the structure adopted in the solid state may differ from that in the gas phase and so compounds that appear unsuitable for CVD may in fact be feasible precursors. Overall, this study has provided information that can be used to aid the design of precursor molecules for a range of technologically important materials.

Compounds **1–11** were typically isolated from the 1:1 reaction of MR_3 with R′OH. However, reaction of $GaEt_3$ with an excess of $HOCH_2CH_2NMe_2$ in refluxing toluene resulted in the isolation of a 1:1 mixture of **2** and the gallium bis-alkoxide $[EtGa(OCH_2CH_2NMe_2)_2]$ (**15**) [34] after sublimation. X-ray crystallography showed that **15** was monomeric with the gallium atom adopting a distorted trigonal bipyramidal geometry, with the oxygen atoms of each alkoxide and an ethyl ligand occupying the three equatorial positions and the N atoms of the NMe_2 group in the axial positions (Fig. 6). Compound **15** represented the first structurally characterized gallium bis-alkoxide and previous attempts to isolate gallium bis-alkoxides incorporating simple monofunctional alcohols had so far been unsuccessful. The requirement to reflux for >24 h to enable formation of **15** in combination with **2**, suggests that the AACVD reactions of MR_2/R′OH in toluene only produces the monoalkoxides, $[R_2M(OR')]_2$ in situ since the AACVD bubbler remains at room temperature. Unfortunately, compound **15** could only be isolated as a mixture with **2**, however the direct synthesis of gallium bis-alkoxides can be achieved from the reaction of $[Ga(NMe_2)_2Cl]$ and two equivalents of R′OH to yield compounds of the type $[ClGa(OR')_2]$ (R′ = $CH_2CH_2NMe_2$, $CH(CH_3)CH_2NMe_2$) [43]. Alternatively, the addition of excess $HOCH(CH_3)CH_2NMe_2$ to $[Me(Cl)Ga\{N(SiMe_3)_2\}]_2$ has been shown to yield the monomeric gallium bis-alkoxide, $[MeGa(OCH(CH_3)CH_2NMe_2)_2]$ [44].

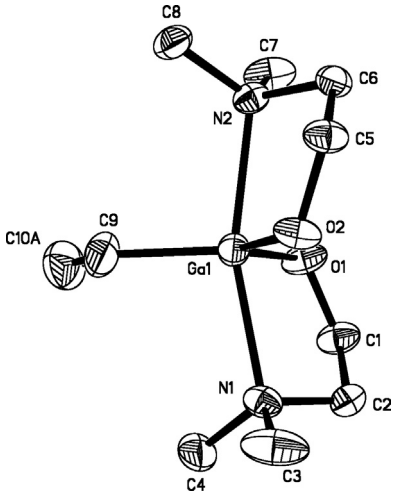

Fig. 6. X-ray structure of compound **15** with thermal ellipsoids shown at the 50% probability level (hydrogen atoms omitted for clarity).
Reprinted with permission from Ref. [34]. Copyright 2004 Royal Society of Chemistry.

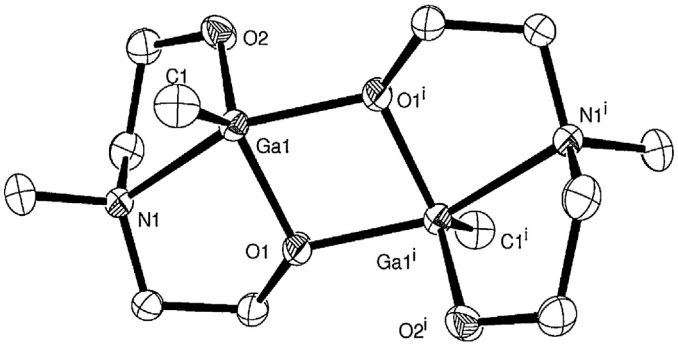

Fig. 7. X-ray structure of compound **18** with thermal ellipsoids shown at the 50% probability level (hydrogen atoms omitted for clarity).
Reprinted with permission from Ref. [47]. Copyright 2012 Wiley.

The related homoleptic gallium tris(alkoxides) $[Ga(OR)_3]_n$, incorporating donor functionalized alcohols, were prepared by the reaction of $[Ga(NMe_2)_3]_2$ and excess R′OH (R′ = $CH_2CH_2NMe_2$, $CH(CH_3)CH_2NMe_2$, $C(CH_3)_2CH_2OMe$, CH_2CH_2OMe) in toluene at room temperature. These compounds could only be isolated as oils, which could be advantageous for CVD and thin films of Ga_2O_3 were produced from the in situ AACVD reaction of $[Ga(NMe_2)_3]_2$ and R′OH in toluene at 550 °C. The films produced were amorphous, transparent and displayed high transmission (80–90%). Annealing the films in air at 600 °C did not result in crystalline films, as expected, but WDX indicated that the annealed films had the composition Ga_2O_3, in contrast to the oxygen deficient (Ga:O 1:1.15) as-deposited films. Gas sensing experiments showed that the films displayed an *n*-type response, albeit low, to ethanol at a range of temperatures [45]. These films were comparable to those deposited from GaR_3/R′OH with good substrate coverage although the as-deposited films were oxygen deficient.

2.2. Multidentate alkoxides

With heteroleptic gallium alkoxides, one co-ligand that has received very little attention is hydride (H^-). Gallium hydride complexes are low mass (hence volatile) and are expected to have a clean decomposition path, owing to the thermodynamic weakness of the Ga—H bond. For example, gallane itself $[\{GaH_3\}_2]$ is highly unstable, decomposing to gallium metal and hydrogen at −30 °C [46]. We synthesized gallium hydride complexes stabilized by multidentate alkoxides (Scheme 3) and investigated their viability as precursors to thin films of Ga_2O_3 by both AACVD and LPCVD [47]. Reaction of $[Me_{3-x}N(CH_2CH_2O)_x]$ (**L^x**; $x = 1, 2$) with $[GaH_3(NMe_3)]$ yielded the multidentate alkoxides $[H_2Ga(OCH_2CH_2NMe_2)]_2$ (**16**) and $[HGa\{(OCH_2CH_2)_2NMe\}]_2$ (**17**) and the ^{1}H NMR of both compounds contained a broad peak at 5.21 and 5.15 ppm, respectively, characteristic of gallium hydride signals. The yield of **16** was improved by the direct reaction of the hydrochloride salt of ligand **L^1** with $LiGaH_4$, however, compound **17** could not be isolated via this route since decomposition and the formation of gallium metal occurred.

In order to directly compare the suitability of methyl groups and hydride ligands in CVD precursors, the synthesis of the related methyl-derivative of **17** was also investigated. Reaction of one equivalent of **L^2** with $GaMe_3$ resulted, after work-up, in the isolation of $[MeGa\{(OCH_2CH_2)_2NMe\}]_2$ (**18**) in high yield. Single-crystal X-ray analysis of **18** (Fig. 7) showed that the compound existed as an oxygen-bridged dimer. Each gallium centre was shown to adopt a five-coordinate environment with the τ value of 0.48 indicating that neither a square-based pyramidal nor a trigonal bipyramidal description is appropriate and in fact the compound exists almost exactly half-way between the two ideals [48].

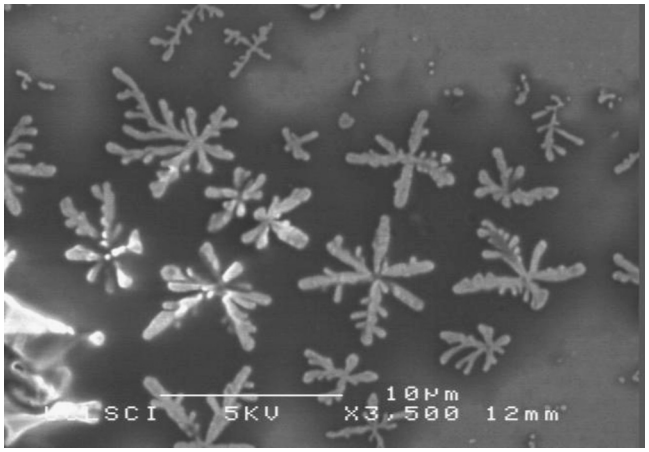

Fig. 8. SEM images for Ga_2O_3 films deposited via AACVD from compound **19** at 450 °C showing the morphology of the region of the film underneath the wires.
Reprinted with permission from Ref. [47]. Copyright 2012 Wiley.

TGA of compounds **17** and **18** indicated that, although they were similar, the onset of mass loss was significantly lower for the hydride derivative (100 °C for **17** and 190 °C for **18**) suggesting that this compound would be an excellent precursor with high thermal stability and volatility. Surprisingly, attempts at using the precursors in a low pressure CVD technique only resulted in decomposition. AACVD of **17** and **18** in toluene solution at 450 or 550 °C did, however, yield transparent thin films of Ga_2O_3. Although, a related homoleptic compound, $[Ga(OCH_2CH_2NMe_2)_3]$ (**19**), prepared via the reaction of **17** with one equivalent of $Me_2NCH_2CH_2OH$, formed superior films of Ga_2O_3 via AACVD. The films deposited from **19** were transparent, adherent and had good coverage over the majority of the glass substrate. The band gap for these films were calculated at 4.6 eV in good agreement with literature values of ~4.9 eV and after annealing, powder XRD confirmed formation of the monoclinc β-phase of Ga_2O_3. These films also had an interesting snowflake-like morphology (Fig. 8) and wire-type deposits near the aerosol inlet.

2.3. Sesquialkoxides

Group 13 sesquialkoxides are tetrameric compounds, which possess a M:O ratio of 2:3, the desired ratio for the metal oxides, M_2O_3. Thus, complexes of this type represent ideal precursors to group 13 oxides. Prior to our work, the formation of Al_2O_3 using an aluminium sesquialkoxide was described, although limited details were reported [49]. The synthesis of sesquialkoxides usually involves a ligand redistribution reaction between metallanes and earth metal alkoxides. However, we investigated the reaction of $GaMe_3$ and $InMe_3$ with 4-methylbenzyl alcohol (4-$MeC_6H_4CH_2OH$) in a 4:9 ratio, which resulted in the isolation of two different types of sesquialkoxides $[Ga\{MeGa(OCH_2C_6H_4Me\text{-}4)_3\}_3]$ (**20**) and $[In\{Me_2In(OCH_2C_6H_4Me\text{-}4)_2\}_3]$ (**21**), according to Scheme 4 [50]. The crystal structure of **20** was shown to consist of a central Ga^{3+} ion coordinated by three $[MeGa(OCH_2C_6H_4Me\text{-}4)(\mu\text{-}OCH_2C_6H_4Me\text{-}4)_2]^-$ units. Thus, the central Ga atom in **20** is six coordinate with three four coordinate Ga atoms occupying the periphery. This arrangement results in the central Ga atom being chelated in a bidentate fashion through two oxygen atoms of the three $[MeGa(OCH_2C_6H_4Me\text{-}4)(\mu\text{-}OCH_2C_6H_4Me\text{-}4)_2]^-$ units.

The structure of **21** was not determined as X-ray-quality crystals could not be obtained. However, ^{1}H NMR of **21** showed the presence of only one set of resonances for the aromatic protons in $OCH_2C_6H_4Me$-4 and the methyl group in $OCH_2C_6H_4$*Me*-4 and one for the In-Me group, indicating the formation of a

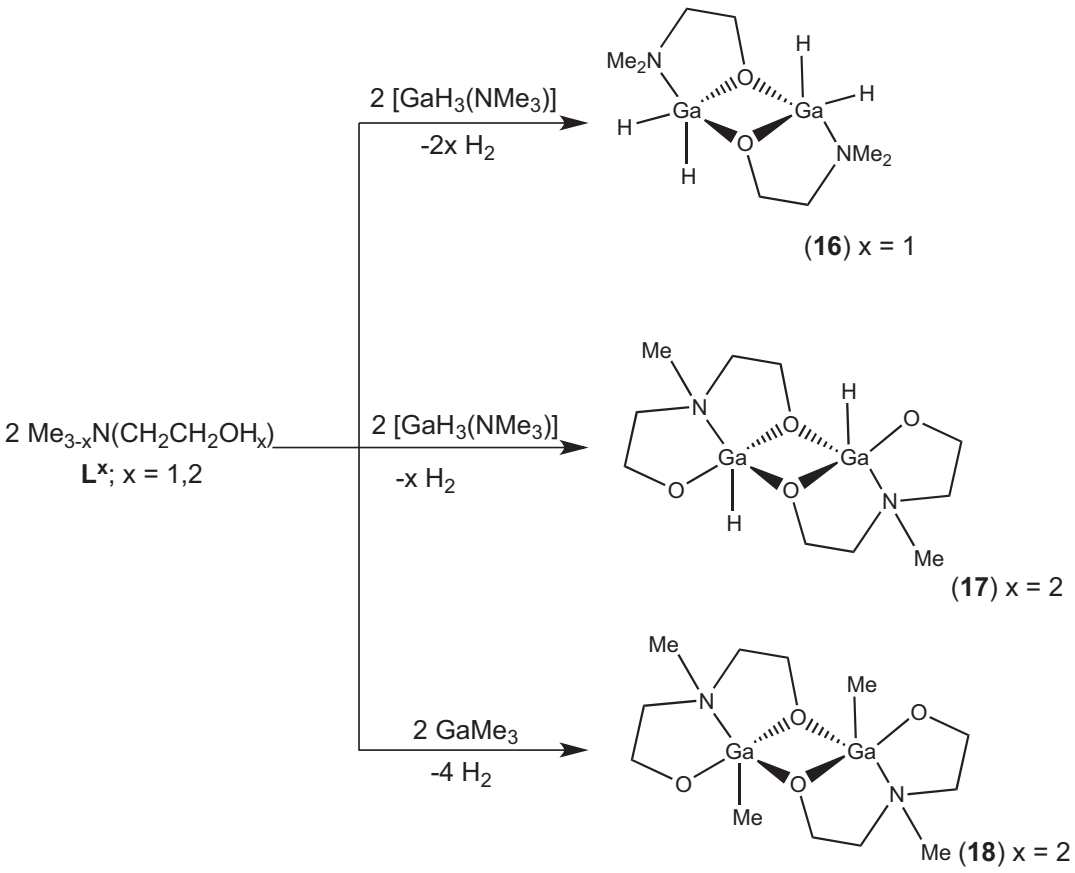

Scheme 3. Synthesis of compounds **16**–**18** [47].

symmetrical structure rather than the same type of sesquialkoxide as observed for the gallium complex **20** (Scheme 4). The formation of the two different sesquialkoxides for Ga and In was related to differences in the reactivity of $GaMe_3$ versus $InMe_3$, where the more reactive $GaMe_3$ afforded the unsymmetrical sesquialkoxide $[Ga\{MeGa(OCH_2C_6H_4Me\text{-}4)_3\}_3]$, whereas the less reactive $InMe_3$ yielded the symmetrical sesquialkoxide $[In\{Me_2In(OCH_2C_6H_4Me\text{-}4)_2\}_3]$.

Since compound **20** possesses the correct ratio of Ga:O atoms (2:3), at the core of the molecule, for that found in gallium oxide (Ga_2O_3) its use as a single-source precursor was investigated. LPCVD of **20** resulted in the deposition of crystalline Ga_2O_3 films at 600 °C. Thus, powder XRD of the film obtained from **20** showed a diffraction pattern consistent with the formation of monoclinic β-Ga_2O_3 with lattice parameters of $a = 12.26(2)$ Å, $b = 3.038$ Å, and $c = 5.81(1)$ Å. These results were surprising, as Ga_2O_3 films are typically only crystalline above 700 °C and could be due to the careful design of the precursor such that the correct ratio of Ga:O atoms (2:3) was present at the core of the molecule.

2.4. β-Diketonates and β-ketoiminates

Another group of compounds which have found use as precursors to thin films of M_2O_3 are the homoleptic group 13 tris(β-diketonates). These compounds, of general formula $[M(bdk)_3]$ (bdk = β-diketonate) are monomeric, 6-coordinate octahedral compounds (Fig. 9). By far the most commonly used is $[Ga(acac)_3]$ (acac = acetylacetonate), which is commercially available, but $[Ga(hfac)_3]$ (hfac = 1,1,1,5,5,5-hexafluoroacetylacetonate) has also found use as a precursor [51,52]. In an attempt to form indium oxide films we investigated the AACVD of a suspension of $[In(thd)_3]$ (thd = 2,2,6,6-tetramethylheptane-3,5-dionate) in CH_2Cl_2 at 450 °C.

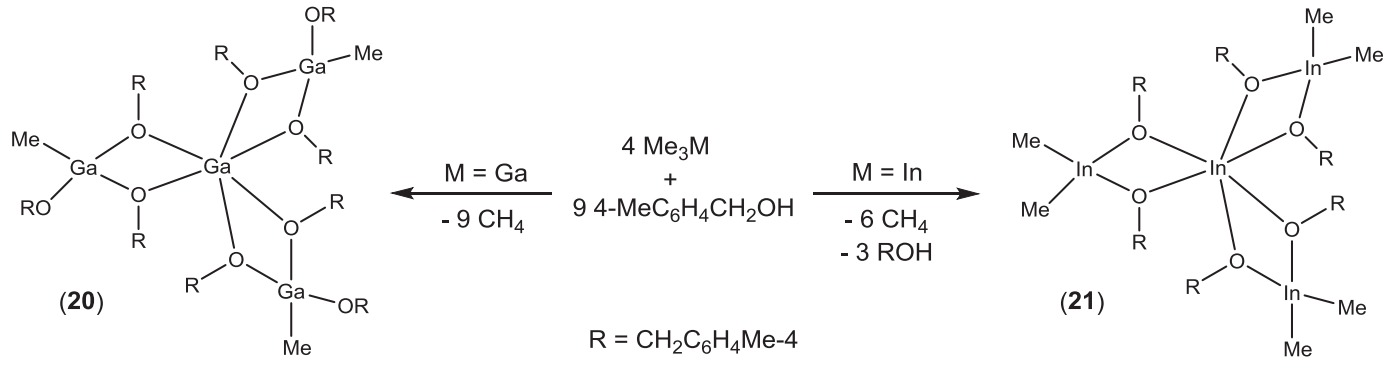

Scheme 4. Synthesis of compounds **20** and **21** [50].

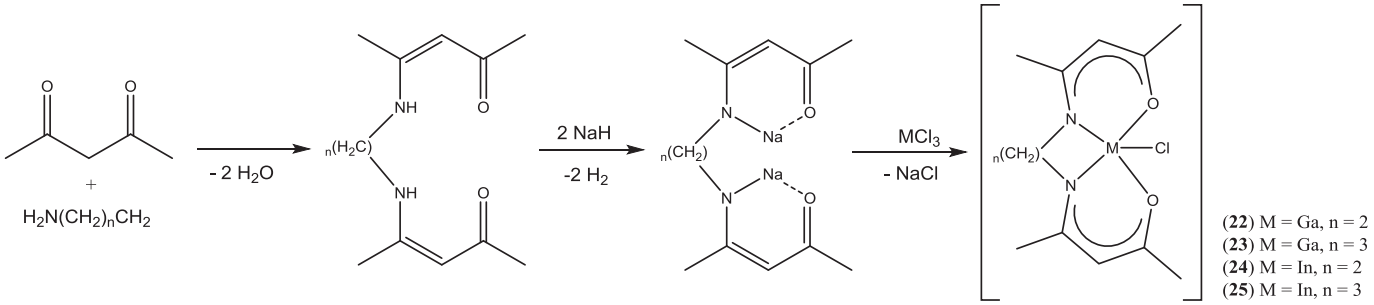

Scheme 5. Synthesis of compounds **22**–**25** [55].

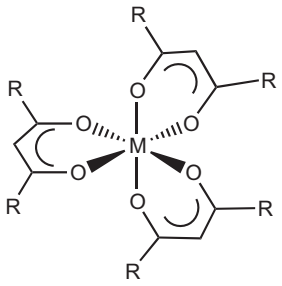

Fig. 9. General structure of [M(bdk)$_3$] (bdk = β-diketonate).

Thin crystalline films of indium oxide were deposited but efforts to grow thicker films were hampered by the poor solubility of [In(thd)$_3$], so the synthesis of heteroleptic compounds of the type [M(bdk)$_2$X] (M = Ga, In; bdk = β-diketonate; X = Cl, H, Me) was attempted such that the solubility could be improved by tuning the ligands surrounding the metal centre. Mono(β-diketonates), such as [GaMe$_2$(acac)] [53], are known compounds but have not been used as precursors to Ga_2O_3, whereas the only bis(β-diketonate) known is an involatile ion pair, [Ga(acac)$_2$(thf)$_2$]$^+$[GaCl$_4$]$^-$, thus is unsuitable for CVD purposes [54,53]. However, all attempted syntheses of gallium bis(β-diketonate) compounds resulted in the isolation of homoleptic [Ga(bdk)$_3$] complexes and similar results were obtained for indium. This was thought to be due to the high kinetic and thermodynamic stability of [M(bdk)$_3$] (M = Ga, In) and the facile rearrangement of any intermediates, of the type [GaX(bdk)$_2$] to the extremely stable homoleptic gallium β-diketonates.

The β-ketoiminate ligand offers a potential means to address the aforementioned problems of volatility and solubility since there is the ability to functionalize the imino residue of the ligand. The thermal stability and solubility of the precursor can be increased by tuning the groups attached to the nitrogen atom on the β-ketoiminate ligand. In turn, the isolation of monomeric species with high vapour pressures could be achievable, particularly if hydride is used as the 'co-ligand'. A further advantage of employing this type of ligand is the potential to enhance surface reactions between the metal β-ketoiminates and the surface of the substrate. We therefore investigated the synthesis of new β-ketoimine ligands (and their sodium salts) and studied their reactivity with a range of group 13 species including chloride, alkyl and hydride compounds [55].

The *bis*(β-ketoimine) ligands, [R{N(H)C(Me)CHC(Me) = O}$_2$] (**L$_1$H$_2$**, R = (CH$_2$)$_2$; **L$_2$H$_2$**, R = (CH$_2$)$_3$) are linked by ethylene (**L$_1$**) and propylene (**L$_2$**) bridges and were used to form gallium and indium chloride complexes, of the type [Ga(L$_n$)Cl] (**22** n = 1; **23**, n = 2) and [In(L$_n$)Cl] (**24**, n = 1; **25**, n = 2) as shown in Scheme 5. The *bis*(β-ketoimine) ligands were synthesized via the reaction of acacH with 1,2-diaminoethane or 1,3-diaminopropane and on reaction with NaH afforded the disodium salts of the ligand (Scheme 5). The ^{1}H NMR of **22** showed backbone CH resonances at ca. 5 ppm, ethylene bridge resonances at ca. 3.5 ppm and methyl group peaks ~1.5–2.0 ppm. However, the ^{1}H NMR of the indium analogue, **24**, suggested the presence of two different ligand environments, with

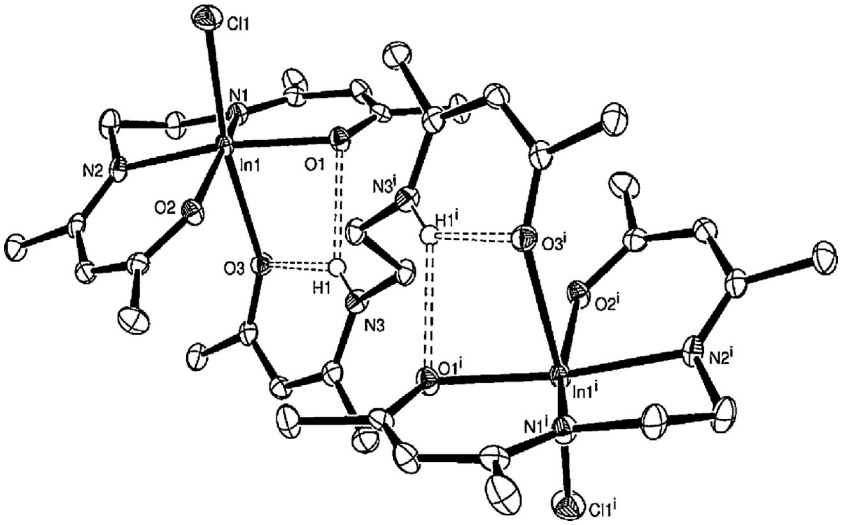

Fig. 10. X-ray structure of compound **24a** with thermal ellipsoids shown at the 50% probability level (hydrogen atoms omitted for clarity). Reprinted with permission from Ref. [55]. Copyright 2012 American Chemical Society.

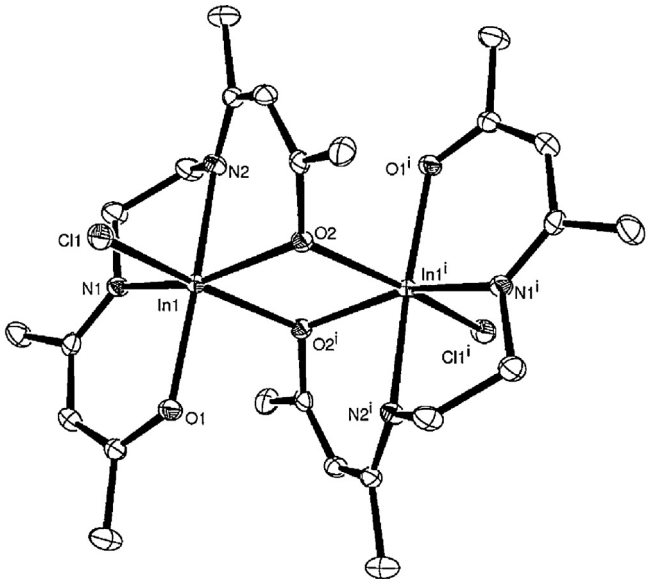

Fig. 11. X-ray structure of compound **24** with thermal ellipsoids shown at the 50% probability level (hydrogen atoms omitted for clarity).
Reprinted with permission from Ref. [55]. Copyright 2012 American Chemical Society.

one set of resonances being close to that of the free ligand (including an NH peak at 10.98 ppm) and the other set corresponding to coordinated ligand in a 1:2 ratio.

The solid-state structure of **24** was determined and showed that ligand $\mathbf{L_1}$ had bonded to indium in the expected manner (Fig. 10) through both oxygen atoms and both nitrogen atoms, with a chloride ligand also attached. However, instead of the anticipated five-coordinate indium complex, a six-coordinate octahedral species (**24a**) was formed with one equivalent of $\mathbf{L_1H_2}$ bridging between two In centres through ketone oxygens. The extra equivalent of $\mathbf{L_1H_2}$ was thought to result from incomplete reaction of $\mathbf{L_1H_2}$ with NaH prior to the in situ addition of $InCl_3$. Reaction of an isolated sample of the salt, Na_2L_1, with $InCl_3$ yielded a product, the ^1H NMR of which showed only one set of ligand resonances. The solid-state structure confirmed that there was no extra ligand bridging between the two metal centres, however, the complex existed as an oxygen-bridged dimer (Fig. 11). The formation of a dimer is most likely due to the inflexibility of the 2-carbon bridge in ligand $\mathbf{L_1}$, which enables a sixth donor group to coordinate to the vacant site (via dimerization) due to $\mathbf{L_1}$ not occupying a sufficient amount of the coordination sphere at indium. Indeed, a thf adduct of $[In(L_1)Cl]$ was also isolated and structurally characterized.

The compounds, $[Ga(L_2)Cl]$ (**23**) and $[In(L_2)Cl]$ (**25**) were also synthesized and structurally characterized. Both complexes adopted five-coordinate monomeric structures, as shown in Fig. 12, with broad resonances in the ^1H NMR of both compounds suggesting fluxional behaviour of the molecules in solution. Some related work was published at a similar time to our report [56].

A key aim of synthesizing the gallium and indium β-ketoiminates was to develop a range of highly volatile precursors for use in CVD. Therefore, the chloride complexes **22** and **24** were reacted with a range of hydride sources (LiH, NaH, $NaBH_4$, $LiBH_4$, $NaBEt_3H$) in attempt to replace the chloride ligand with a hydride. Unfortunately, in all cases no reaction was observed and only the starting material remained. However, reaction of $\mathbf{L_1H_2}$ with a freshly prepared ethereal solution of $[GaH_3(NMe_3)]$ yielded the hydrido gallium β-ketoiminate, $[Ga(L_1)H]$ (**26**, Scheme 6) in good yield. Although single crystals could not be isolated, the formation of **26** was confirmed by analytical and spectroscopic techniques and in particular a peak was observed at 5.56 ppm in the ^1H NMR, which is characteristic of gallium hydrides. In contrast, the analogous indium hydride could not be isolated and attempts to form the compound only resulted in decomposition to indium metal.

We then turned our attention to the synthesis of gallium and indium β-ketoiminates incorporating an extra Lewis base, i.e. donor-functionalized β-ketoiminates. Coordinative saturation of the metal centre should be possible due to the presence of the extra Lewis base allowing for the isolation of additional hydride species. Therefore, the β-ketoimine ligand $[Me_2N(CH_2)_3N(H)C(R)CHC(R)=O]$ ($\mathbf{L_3H}$, R = Me; $\mathbf{L_4H}$, R = Ph) were synthesized and used to form the gallium and indium alkyl complexes, $[Ga(L_3)Me]$ (**27**) and $[In(L_3)Me]$ (**28**), and the gallium hydride compounds $[Ga(L_n)H]$ (**29**, $n=3$; **30**, $n=4$), as shown in Scheme 7.

The β-ketoiminate gallium hydride compounds (**26** and **29**) have been used as single-source precursors for the deposition of Ga_2O_3 films by AACVD with toluene as the solvent. The quality of the film varied with compound **26** being the superior precursor, affording transparent (transparency ranging from 80 to 90% in the visible), adherent films, Fig. 13. The deposition of transparent films from **26** is in contrast to films deposited from $[Me_2Ga(OR')]_2$, described in Section 2.1, which typically resulted in the deposition of grey or brown films indicative of carbon contamination probably due to the retention of carbon from the Ga—C bond. The lower

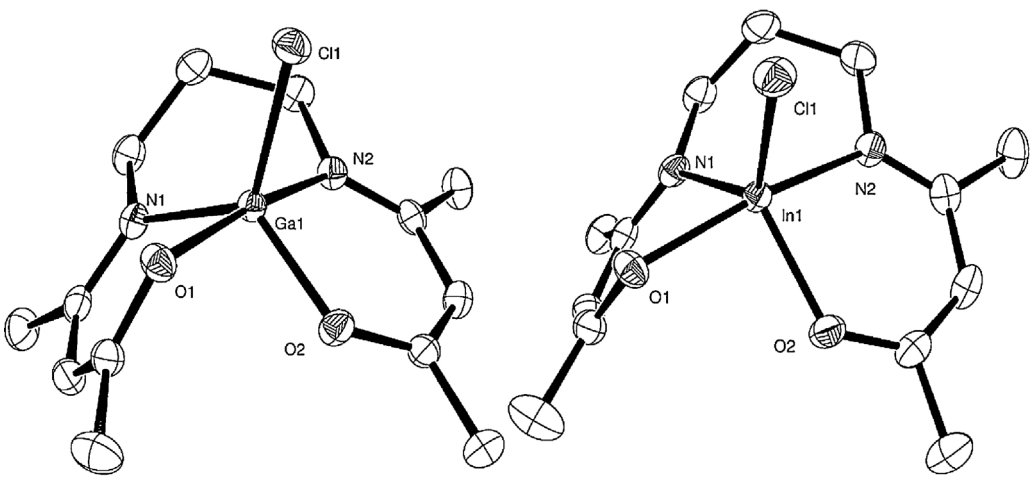

Fig. 12. X-ray structure of compounds **22** and **25** with thermal ellipsoids shown at the 50% probability level (hydrogen atoms omitted for clarity).
Reprinted with permission from Ref. [55]. Copyright 2012 American Chemical Society.

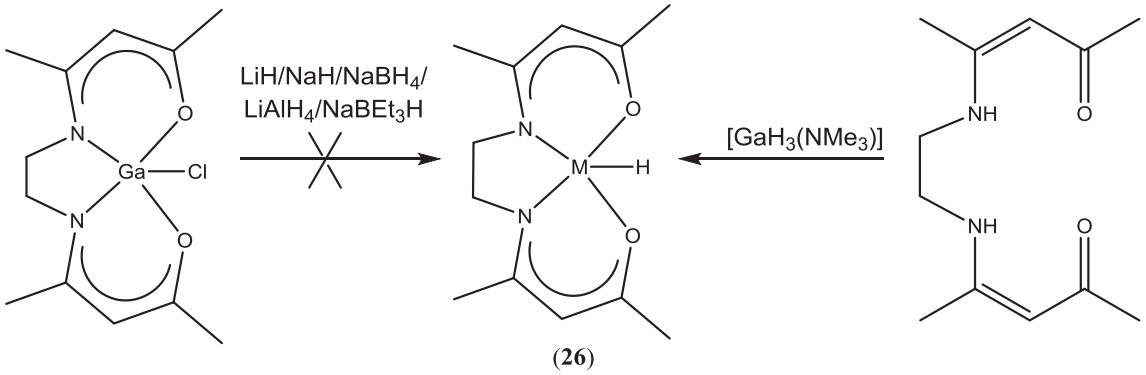

Scheme 6. Synthesis of compound **26** [55].

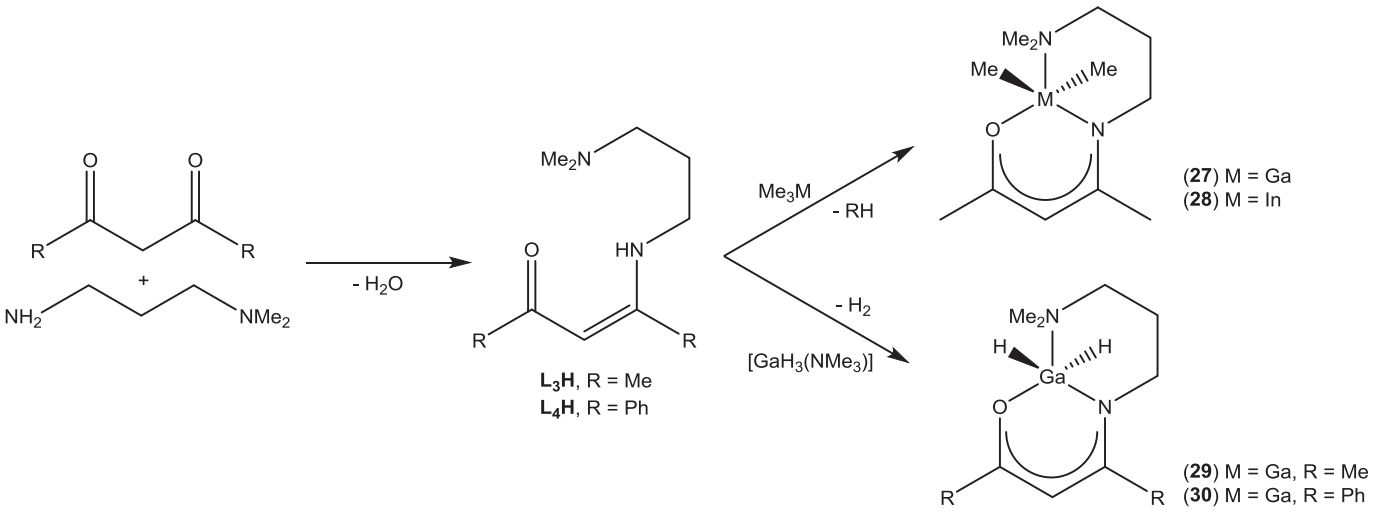

Scheme 7. Synthesis of compounds **27**–**30** [55].

carbon contamination in films deposited from **26** could be attributed to the presence of the hydride ligand in the compound in place of alkyl groups resulting in minimal contamination. As expected the films were amorphous as deposited but they could be annealed at 1000 °C to form crystalline Ga_2O_3.

2.5. Gallium-doped indium oxide

Interest in TCOs over the past two decades has increased dramatically due to their application in optoelectronic devices such as flat panel displays, solar cells and photovoltaics. In order to improve TCO film optical, electrical and chemical properties a range of studies have focused on doping various metal oxide combinations of In, Sn, Al, Zn and Ga. Gallium-indium-oxide is the reported parent phase of a promising, relatively unexplored TCO family. An advantage that gallium-indium-oxide has over ITO is its improved transmission in the blue-green region of the electromagnetic spectrum and the absolute transparency has been shown to rival or exceed that of most TCOs known [12]. Based on the successful deposition of gallium and indium oxide from the precursors described in Sections 2.1–2.3 via AACVD we investigated the use of this technique to afford gallium-doped indium oxide films [57].

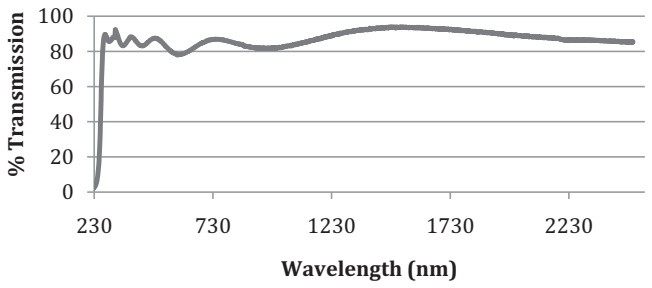

Fig. 13. Vis/IR transmission spectra of a film obtained by AACVD of a toluene solution of **26**.
Reprinted with permission from Ref. [55]. Copyright 2012 American Chemical Society.

Transparent gallium-indium-oxide films were deposited from the in situ AACVD reaction of $GaMe_3$, $InMe_3$, and the donor-functionalized alcohol $HOCH_2CH_2OMe$ in toluene at 450 °C (Scheme 8). The in situ reaction was thought to generate the dimethylalkoxometallane precursors, of the type

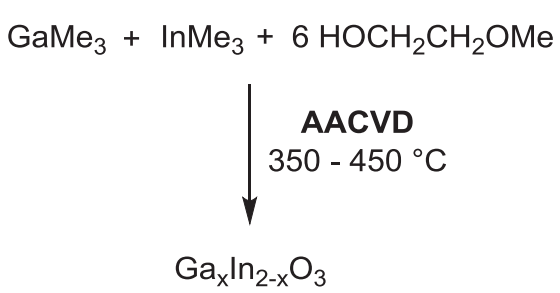

Scheme 8. AACVD reaction of $GaMe_3$, $InMe_3$ and $HOCH_2CH_2OMe$ [57].

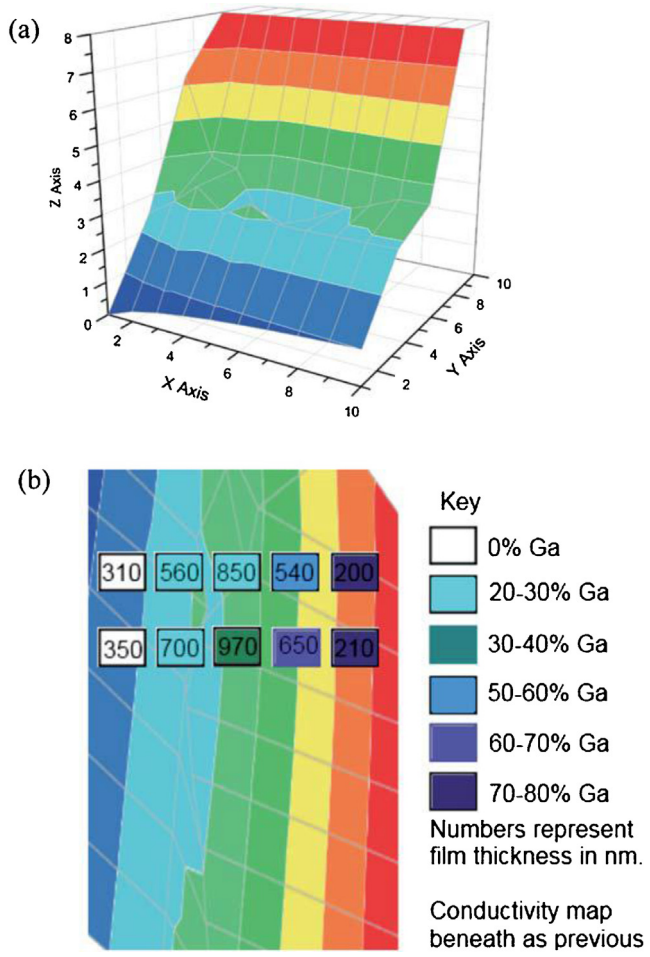

Fig. 14. (a) Conductivity plot of a typical film of graded composition deposited via cAACVD – low conductivity (red) to high conductivity (blue); (b) composition map of gallium-indium-oxide film deposited via cAACVD showing the conductivity, composition and thickness of the film.

Reprinted with permission from Ref. [58]. Copyright 2012 Royal Society of Chemistry.

$[Me_2M(OCH_2CH_2OMe)]_2$, described in Section 2.1 in solution. This is one of the primary advantages of AACVD in that the precursors can be formed and used in situ without the need for isolation and purification. The as-deposited films were amorphous, which is typical for films of gallium oxide deposited at these temperatures, however, indium oxide films are usually crystalline at 450 °C. Thus, the presence of gallium in these films has resulted in the formation of amorphous films. Annealing the films at 1000 °C resulted in highly transparent films and powder XRD showed that a Ga-substituted cubic In_2O_3 microstructure was adopted with a reduced lattice parameter of $a = 9.84$ Å (undoped In_2O_3 $a = 10.81$ Å).

EDXA and WDX analysis showed that the as-deposited and annealed films had the same composition ($Ga_{0.6}In_{1.4}O_{3.1}$). It is interesting to note that less gallium than indium has been incorporated despite the same Ga:In ratio being used in the precursor mix in all film depositions. It is possible that the high temperature favours the formation of a gallium-substituted In_2O_3 framework (rather than a indium-substituted Ga_2O_3 framework) or some gallium gets vaporized. The films were conductive with a sheet resistivity $R_s = 83.3\ \Omega$/square and exceptionally low electrical resistivity, for example, $6.66 \times 10^{-4}\ \Omega$ cm for a 80 nm thick film. In addition, Kelvin probe measurement found the work function of the film was 4.6 eV, which is comparable to ITO and therefore this

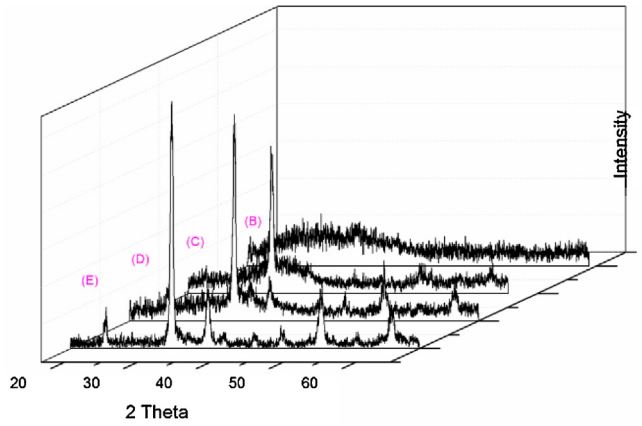

Fig. 15. XRD patterns collected across a film deposited on glass via cAACVD from $GaMe_3/HOCH_2CH_2OMe$ and $InMe_3/HOCH_2CH_2OMe$ both in toluene at 400 °C. The XRD patterns along show amorphous Ga_2O_3 (B); $Ga_xIn_{2-x}O_3$ (C)–(D); In_2O_3 (E).

Reprinted with permission from Ref. [58]. Copyright 2012 Royal Society of Chemistry.

represents a facile method for the formation of alternative TCO films to ITO, without the necessity of oxygen carrier gas.

2.6. Combinatorial CVD of gallium indium oxide

A major goal of materials research has been the development of high-throughput methods for the rapid discovery and optimization of processing routes and recently we reported on a novel combinatorial AACVD (cAACVD) technique to deposit gallium-indium oxide thin films [58]. This new technique combines the advantages of AACVD (volatility/thermal stability restrictions removed) with those of the previously reported combinatorial atmospheric pressure CVD and combinatorial LPCVD (rapid deposition/analysis of a compositional gradient) [59,60]. Films were deposited via cAACVD at 400 °C by overlapping parallel aerosol streams of $InMe_3/HOCH_2CH_2OMe$ in toluene and $GaMe_3/HOCH_2CH_2OMe$ in toluene to from a combinatorial spread of phases across the glass substrate (Fig. 14). This resulted in the formation of a film of metal oxide, with strips of In_2O_3 and Ga_2O_3 on either side of the substrate and a mixed $Ga_xIn_{2-x}O_3$ section in the centre where the aerosol streams overlap. It is likely that the precursors within the AACVD bubblers are species of the type $[Me_2Ga(OCH_2CH_2OMe)]_2$ and $[Me_2In(OCH_2CH_2OMe)]_2$ based on the solution studies described in Section 2.1.

The changing nature of the gallium-indium oxide films across the surface was confirmed by the powder X-ray (XRD) patterns taken across the film (Fig. 15). Closest to the gallium inlet the area was amorphous, consistent with the formation of amorphous Ga_2O_3. However, nearest to the indium inlet crystalline In_2O_3 was observed which was indexed to cubic In_2O_3 with a lattice parameter, $a = 10.091$ Å. EDXA suggested that the intermediate regions of the film had $Ga_xIn_{2-x}O_3$ ($x = 0.4$–1.6) compositions which were found to also be crystalline by XRD. These areas were found to crystallize in the same space group (*Ia*3) as In_2O_3 but with a reduced lattice parameter ($a = 10.066$–10.057 Å with greater gallium doping) consistent with partial substitution of indium ions with the smaller gallium ion causing a reduction in the unit cell.

SEM images of the combinatorial films showed a change in morphology with composition such that the amorphous Ga_2O_3 regions consisted of spherical uniform clusters agglomerated together. In contrast, SEM of the regions of crystalline In_2O_3, showed the formation of crystallites of size ~125 nm in length. The band gap of the films varied from 3.71 to 4.59 eV, as the amount of gallium doping

increased (band gap of Ga_2O_3 ~4.7 eV and In_2O_3 ~3.7 eV). Furthermore, conductivity measurements showed that the area of the film closest to the gallium inlet was insulating, suggesting the formation of Ga_2O_3, which is consistent with the EDXA and XRD data. However, the film became increasingly conductive across the compositional gradient towards the indium inlet, consistent with the formation of $Ga_xIn_{2-x}O_3$ and In_2O_3.

Previous combinatorial CVD routes, including both low pressure and atmospheric methods, have thus far only used simple, volatile precursors, such as metal nitrates and halides. Thus, both techniques require volatile precursors with low decomposition temperatures. To achieve all of the necessary precursor requirements, including high vapour pressure, low decomposition temperature and similar deposition chemistry, for some materials, such as doped-indium oxide, it is difficult. By using a liquid–gas aerosol, as is employed in combinatorial AACVD, the restrictions of thermal stability and volatility are lifted and so new precursors and materials can be investigated, such as for the formation of doped-indium oxide films.

2.7. Transition metal-doped indium oxide

Indium oxide can be doped with other metals to enhance its electronic properties, for example ITO has an optical band gap of 3.4 eV and is widely used in optoelectronic devices. Indium oxide has also been doped with tantalum and titanium by sputtering methods and the resulting films showed improved properties, such as transparency and conductivity. Indium oxide films have also been investigated as gas sensors and currently there is a pressing need to develop new gas sensing materials as the commonly used material, tin dioxide SnO_2, suffers from humidity interference and baseline drift [61]. We therefore investigated doping indium oxide with titanium and tantalum using an AACVD method and the type of precursors described in Section 2.1 [22].

Titanium- and tantalum-doped indium oxide films were deposited on glass via the AACVD reaction of $InMe_3$ and $HOCH_2CH_2NMe_2$ and $M(NMe_2)_x$ ($x = 4$, M = Ti; $x = 5$, M = Ta) and $HOCH_2CH_2NMe_2$ (Scheme 9) in toluene at 400–450 °C. These reactions were assumed to generate the metal alkoxide precursors in situ, of the type $[Me_2InOOCH_2CH_2NMe_2]_2$ and $[M(OCH_2CH_2NMe_2)_x]$. The resulting doped-indium oxide films, In_2O_3:M, were found to contain 6.5 and 2.3 at.% of Ti and Ta, respectively. Powder XRD showed that the films were crystalline and adopted the cubic In_2O_3 bixbyite phase with strong reflections from the (2 2 2) plane and preferred orientation along this plane which is common for thin films of indium oxide. However a notable difference was observed in the shifting of the peak positions (in comparison to undoped In_2O_3 films) and this, along with the absence of any additional peaks suggests direct substitution of the In^{3+} cations with Ti^{4+} and Ta^{5+} ions in the crystal matrix. The doped films showed minimal reflectivity ~10% and high transmission (75–85%) compared to plain glass substrates (80–90%).

The gas sensing properties were investigated on films deposited onto gas sensing substrates via the same AACVD procedure. Gas sensing responses were tested to reducing (ethanol, carbon monoxide, butane and ammonia) and oxidizing (nitrogen dioxide) gases. The films showed no sensitivity to butane and small responses to the others. However, the tantalum doped indium oxide (In_2O_3:Ta) thin films showed a superior response, compared to In_2O_3, to a number of reducing gases (ethanol, CO, ammonia) and also the oxidizing gas NO_2. Considerable selectivity to ethanol was observed; the greatest gas response (gas response was measured as the ratio between R (the resistance of the film at the point immediately prior to exposure to ethanol) and R_0 (the resistance when exposed to ethanol)) was 16.95–100 ppm ethanol (Fig. 16). These results illustrate how doping can affect the gas sensing properties of the films

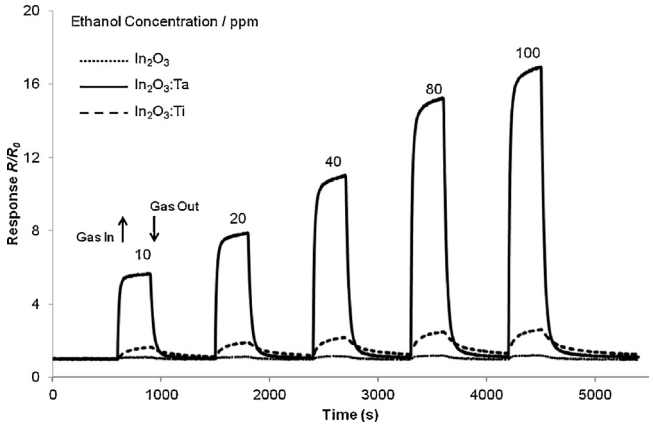

Fig. 16. Gas response (R/R_0) of In_2O_3 sensors upon exposures to differing concentrations of ethanol in flowing air over time at a sensor operating temperature of 500 °C. Arrows indicate when gas flow of ethanol was turned on and off.
Reprinted with permission from Ref. [22]. Copyright 2012 American Chemical Society.

and CVD techniques represent a facile way of preparing metal oxide gas sensors since control over key materials properties such as doping and microstructure can be easily achieved.

3. Precursors to bismuth oxide

Bismuth oxide (Bi_2O_3) has received much interest due to its use as an electrode material in gas sensors [62], an ion conducting electrolyte material in solid oxide fuel cells [63], and as an effective UV light photocatalyst [64]. It is also an important component of several ferroelectric [65], multiferroic [66] and superconducting oxide materials [67]. The band gap of Bi_2O_3 has been reported to be in the range 2.29–3.31 eV depending on the crystalline phase and the optical gap of BiO has been determined to be as high as 3.31 eV, α-Bi_2O_3 to be 2.85 eV and the amorphous phase as low as 2.0 eV [68,69]. These values indicate the potential of Bi_2O_3 to serve as a photocatalyst under solar irradiation. Indeed, the photocatalytic activities of undoped α-, β- and δ-Bi_2O_3 have been demonstrated during degradation of model pollutant dyes, including methylene orange [69] and Rhodamine B7 [64,70]. In addition, transition metal doped γ-Bi_2O_3 nanoparticles have been shown to photocatalytically split water [71].

In general, the availability of volatile single-source bismuth oxide precursors for CVD is limited [72]. In order to deposit phase pure Bi_2O_3 and to overcome the problems of precursor volatility and high deposition temperatures, new single-source precursors are required. The basic requirements for incorporation of oxygen into the molecule using sterically bulky ligands to limit oligomerization have led to the development of three main types of oxygen-containing precursors including alkoxides, β-ketonates and carboxylates. Potential single-source precursors for bismuth oxide have been described in some detail by Mehring in his comprehensive review in 2007 and readers are directed to this review for further information [72]. In this section our contribution to the development of bismuth oxide deposition is described and the section is organized into a single area comprising (i) Alkoxides and β-diketonates.

3.1. Alkoxides and β-diketonates

The decomposition characteristics of $[Bi(O^tBu)_3]$ (**31**), $[Bi(C(CH_3)_2CH_2OMe)_3]$ (**32**) and $[Bi(thd)_3]$ (**33**) were investigated using coupled mass spectrometry-thermal gravimetric analysis-differential scanning calorimetry (MS-TGA-DSC) in order

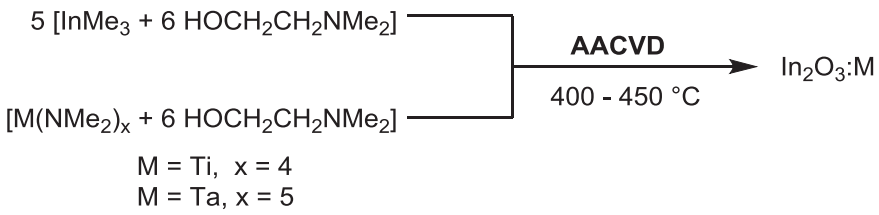

Scheme 9. AACVD reactions in toluene of $InMe_3/HOCH_2CH_2NMe_2$ in the presence of $M(NMe_2)_x/HOCH_2CH_2NMe_2$ to afford In_2O_3:M films [22].

to understand the decomposition pathway of the precursors and therefore identify potential deposition methodology [73]. Compounds **31–33** were prepared using modified literature procedures [74,75]. Compound **31** was shown to exhibit an appreciable vapour pressure (0.48 mmHg, at 100 °C) which was found to be significantly higher than **33** (2.15×10^{-4} mmHg at 100 °C). Although **32** had a higher vapour pressure of 158 mmHg at 100 °C, **31** was shown to have superior decomposition characteristics for the formation of Bi_2O_3, as assessed using TGA. This compound was therefore selected for further deposition studies using LPCVD. The sterically demanding O^{t}Bu groups in **31** inhibit oligomerization of the complex and enhance its volatility.

LPCVD of **31** was studied at temperatures ranging from 425 to 500 °C, at a variety of system pressures and carrier gas flow rates and a relatively low bubbler temperature of 110 °C, required to transport the precursor through the system. Compound **31** proved to be an excellent single-source precursor with clean decomposition to Bi_2O_3 under N_2 giving it a distinct advantage over other commonly used bismuth precursors, which suffer from problems of precursor volatility and high deposition temperatures. XRD showed that the Bi_2O_3 films deposited from **31** consisted of variable mixtures of β- and γ-phases, but at 425 °C, the β-phase was dominant, whereas at 500 °C or upon increasing the carrier gas flow at 450 °C, the γ-phase could be grown preferentially. The morphology of the films was shown to vary with temperature (Fig. 17) using SEM, which also indicated that the films deposited via an island-type growth mechanism. Film thickness increased with respect to substrate temperature and total system pressure. All films possessed band gaps between 2.3 and 3.0 eV dependent upon the phase present and the films displayed excellent photodegradation of water under near-UV irradiation.

In a related study, the moisture stable homoleptic bismuth(III) β-diketonate complex $[Bi(dbm)_3]_2$ (dbm = dibenzoylmethane) was utilized as a single-source precursor to bismuth oxide films via AACVD [76]. In combination with $[H_2PtCl_6.6H_2O]$, platinum nanoparticle-doped bismuth oxide films were afforded on co-deposition with $[Bi(dbm)_3]_2$, yielding Pt–Bi_2O_3 composite films. The introduction of Pt particles into the β-Bi_2O_3 films caused hydrogen to be evolved during photolysis of water over the composite material, a property not found for Pt particles or β-Bi_2O_3 alone.

4. Precursors to transition metal pnictides

Today's society requires ever faster and higher capacity electronic devices. In order to achieve these goals, circuitry must be significantly reduced in size, which in turn means that the barrier layer between interconnects must be smaller and more reliable. In microcircuitry, a conducting barrier layer is essential between the silicon in components and the metal (usually aluminium or copper) connects, as it prevents the diffusion of the metal into the silicon, which would destroy the functionality of the circuit. Currently, TiN is the material of choice for barrier layers where aluminium interconnects are concerned. Titanium nitride (TiN) has a NaCl-type cubic crystal structure with a bulk lattice parameter $a \sim 4.241$ Å ($TiN_{1.0}$). The non-stoichiometric forms, $TiN_{0.42}$–$TiN_{1.2}$, also all have the NaCl cubic structure. Pure $TiN_{1.0}$ films are highly reflective and gold in colour, and have found applications in jewellery and optics [77]. However, synthesis of these golden films is not straightforward, since contamination from carbon and oxygen leads to brown, black or grey colouration. A range of single-source precursors to titanium nitride have been previously reported [78,85].

Tantalum and tungsten nitrides have been shown to be more suited to copper as diffusion barrier materials and are more effective at higher working temperatures [79]. Moreover, tungsten carbonitride is known to be a superior barrier material to copper diffusion in microcircuitry over pure tungsten nitride. Potential precursors to tungsten nitride and carbonitride were discussed in a number of reviews [80,85]. In addition, zirconium nitride is of interest for use in barrier layers as it has a low resistivity of 17–22 μΩ cm at 20 °C. Zirconium carbide adopts a face-centred cubic structure, although the stoichiometries vary widely, ZrC_x ($x = 0.55$–0.99). It has a similar resistivity to the nitride (35–55 μΩ cm at 20 °C) but shows less resistance to chemical attack and it will easily form a solid solution with zirconium nitride as the lattices are similar. Due to their respective resistivities, a solid solution of ZrN and ZrC_x would still be suitable as a barrier layer [81]. There are not many examples of precursors for the CVD of zirconium nitride and compounds that may seem promising for ZrN have instead been used in the presence of oxygen to form ZrO_2 thin films [82].

In contrast to metal nitrides, the formation of titanium phosphide (TiP) thin films has received little attention, although this material possesses a number of useful properties. It is a metallic conductor, refractory (dec. < 1580 °C), hard and shows good resistance to oxidation at elevated temperatures [83]. Furthermore, thin films of early transition metal phosphides have been used as diffusion barriers in semiconductor devices [84]. Metal arsenides are known to exhibit a wide range of functional properties, and display band gap characteristics, which are currently exploited within a range of photonic devices including lasers and light emitting diodes (LEDs). Apart from key III/V materials (e.g. GaAs, InAs), knowledge surrounding metal arsenide thin films, particularly via CVD, remains limited; typically with only bulk material formation known. It is well understood that arsenide compounds are considerably less stable and volatile than their phosphorus counterparts, which has until recently limited research into arsenic containing thin films. However, recent advances within CVD technology and the development of single-source precursors, has now facilitated research into this area.

As the understanding of the roles of the precursor have developed, more user-friendly (i.e. safer and easier to handle) precursors have been introduced that have proved capable of not only depositing at much lower deposition temperatures, but also in producing high quality deposits. We have been studying a range of nitrogen containing metal complexes and assessing their ability to form metal nitride thin films via CVD and have attempted to develop simple phosphine and arsine adducts of titanium(IV) for potential application as single-source precursors to titanium phosphide and arsenide films. CVD routes to metal nitrides, including both single- and dual-source methods, have recently been reviewed in

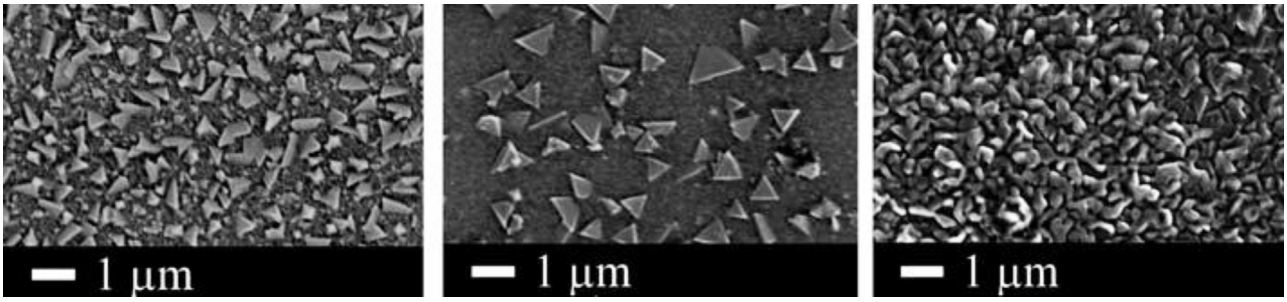

Fig. 17. Scanning electron micrographs of Bi_2O_3 films deposited via LPCVD of $[Bi(O^tBu)_3]$ at 425 °C (left), 475 °C (centre), and 500 °C (right). Reprinted with permission from Ref. [73]. Copyright 2010 Royal Society of Chemistry.

detail [85]. In this section our contribution to the development of transition metal pnictide deposition is described and the section has been organized into 3 areas comprising (i) titanium and zirconium guanidinates, (ii) transition metal imido complexes and (iii) titanium phosphine and arsine complexes.

4.1. Titanium and zirconium guanidinates

Compounds containing guanidinate ligands $\{(R'N)_2CNR_2\}$ have received interest as precursors to metal nitride thin films due to their nitrogen content, ability to stabilize the metal centre due to their electronic flexibility and their potential to increase the volatility of the compound [85,86]. The presence of the NR_2 moiety in these ligands results in the possibility of a zwitterionic resonance structure, as indicated in Scheme 10. Donation from the dialkylamido lone pair into the ligand could result in its metal complexes being electron rich when compared to other ligands, such as amidinates.

The mono(guanidinato) complex $[Ti(NMe_2)_2Cl\{^iPrNC[N(SiMe_3)_2]N^iPr\}]$ (**34**) was prepared by reaction of $[Ti(NMe_2)_2Cl_2]$ with 1 or 2 equiv. of the lithium guanidinate salt $[Li\{^iPrNC[N(SiMe_3)_2]N^iPr\}]$ [87]. In contrast, $[TiCl_2\{^iPrNC(NMe_2)N^iPr\}_2]$ (**35**) was prepared from the reaction of $[Ti(NMe_2)_2Cl_2]$ and 2 equiv. of $^iPrN=C=N^iPr$, according to Scheme 11. A single-crystal structure determination of **34** showed the complex to have a distorted trigonal bipyramidal geometry at the titanium centre, with the metal lying 0.171 Å out of the equatorial plane in the direction of Cl.

LPCVD of either compound **34** or **35** at 600 °C resulted in the deposition of thin highly reflective, conducting gold-coloured films of titanium carbonitride. EDAX of the resulting films showed that the chlorine contamination was below 0.1 atom%. XPS of the films confirmed this and indicated the presence of titanium, nitrogen, carbon, and oxygen. The surface of the film was principally oxide terminated, however, etching into the film surface massively reduced the oxide contamination. Overall films grown from **34** had an approximate composition of $TiC_{0.3}N_{0.7}$, whereas those from **35** were $TiC_{0.5}N_{0.5}$. The films were amorphous according to powder XRD. The films were hard and resistant to scratching, indicating that they were well adhered to the substrate. In addition, they showed some interesting optical properties, such as high optical reflectance as heat mirrors (having less reflectance in the IR region). The formation of titanium carbonitride films from **34** and **35** shows that titanium guanidinate complexes are suitable precursors for titanium carbonitride films.

Two novel zirconium guanidinate precursors, $[ZrCp'\{\eta^2\text{-}(^iPrN)_2CNMe_2\}_2Cl]$ (**36**) and $[ZrCp'_2\{\eta^2\text{-}(^iPrN)_2CNMe_2\}Cl]$ (**37**) (Cp′ = monomethylcyclopentadienyl) were examined as potential precursors to zirconium carbonitride [88]. The synthesis of **36** proceeded via reaction of $[ZrCl_2(NMe_2)_2(THF)_2]$ with the carbodimide $^iPrN=C=N^iPr$ to yield the intermediate compound $[ZrCl_2\{\eta^2\text{-}(^iPrN)_2CNMe_2\}_2]$, which on further reaction with NaCp′ formed **36**. In contrast, precursor **37** was synthesized via a lithium metathesis route in which $[ZrCp'_2Cl_2]$ was synthesized from the reaction of 2 equivalents of NaCp′ and $[ZrCl_2(THF)_2]$ and reacted with the lithium guanidinate salt to afford **37**. The crystal structures of **36** and **37** were determined and in both complexes the Cp′ ligand can be considered to be bound in an η^5 mode (Fig. 18). The structure of compound **36** exhibited a distorted octahedral geometry due to the steric constraints of the guanidinate ligand, assuming the Cp′ moiety occupies one coordination site and the two guanidinate ligands are inequivalent. Both compounds decomposed cleanly, as shown by TGA, although compound **36** showed a lower mass loss than expected, suggesting that full decomposition had not taken place at 590 °C. The clean decomposition and volatility of these compounds indicated their potential for use as CVD precursors.

LPCVD of **36** and **37** resulted in the formation of highly reflective, adhesive, amorphous films of zirconium carbonitride at 600 °C. WDX data for the films deposited indicated that more nitrogen in the single-source precursor resulted in more nitrogen in the film. Thus, the film formed from compound **36**, containing two guanidinate ligands, contained almost three times as much nitrogen as zirconium compared to those deposited from compound **37**, with compositions of $ZrN_{2.80}C_{1.82}$ and $ZrN_{1.31}C_{2.46}$ (from **36** and **37**, respectively). The XRD patterns for films from both precursors showed some polycrystalline ZrC, although the films were assumed to be largely amorphous. Compounds **36** and **37** show potential as precursors to zirconium carbonitride although as much nitrogen as possible should be incorporated into the precursor as shown by the presence of more nitrogen in the films from **36**.

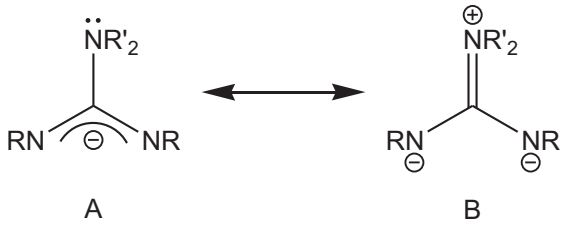

Scheme 10. Canonical forms of guanidinate ligands [84,86].

4.2. Transition metal imido complexes

Thin films have been formed on glass by LPCVD of eleven closely related single-source precursors including, $[TiCl_2(N^tBu)(py)_3]$ (**38**), $[TiCl_2(NC_6F_5)(Me_3[9]aneN_3)]$, $[TiCl_2(N^iPr)(NHMe_2)_2]$, $[TiCl_2(NC_6H_3Me_2\text{-}2,6)(py)_3]$, $[TiCl_2(NC_6H_3{}^tPr_2\text{-}2,6)(py)_3]$, $[TiCl_2(NPh)(NHMe_2)_2]$, $[TiCl_2(N^iPr)(Me_3[9]aneN_3)]$, $[TiCl_2(NC_6F_4H\text{-}4)(NHMe_2)_2]$, $[TiCl_2(N^tBu)(Me_3[6]aneN_3)]$, $[TiCl_2(N^iPr)(Me_3[6]aneN_3)]$ and $[TiCl_2(NC_6H_3Me_2\text{-}2,6)(NHMe_2)_2]$ [89,90]. These compounds were prepared by modification of existing literature

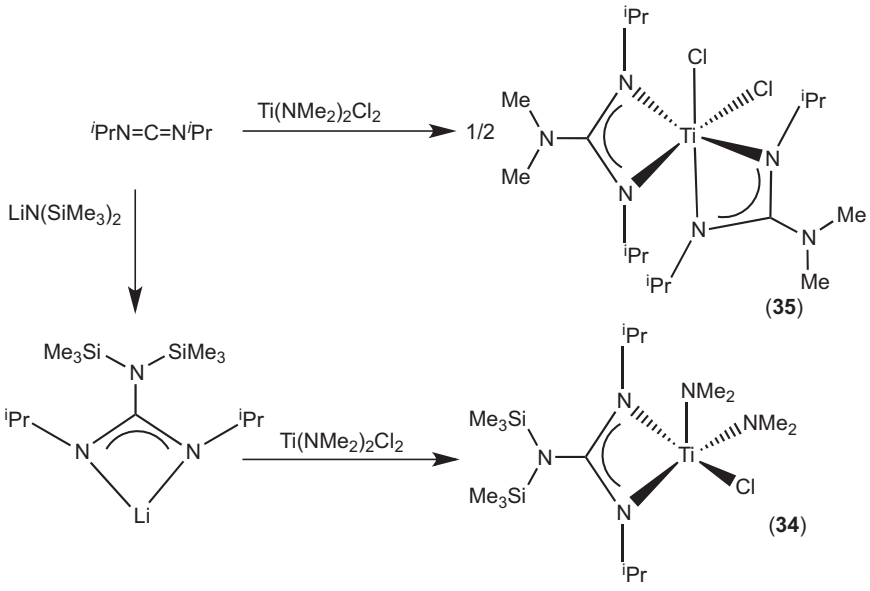

Scheme 11. Synthesis of compounds **34** and **35** [87].

methods [91]. The precursors in this series are all very similar, containing one strong Ti = NR multiple bond, two or three Ti—N dative bonds and two Ti—Cl bonds. Therefore, the geometry around the titanium is either pseudo-octahedral or trigonal bipyramidal.

All the titanium imido compounds deposited thin films under LPCVD conditions at 600 °C and the majority of the precursors formed titanium nitride films, however, bulkier imido complexes and those with chelating ligands produced thin films with significant oxygen and carbon contamination, suggesting incomplete decomposition and post reaction oxidation. The best single-source precursor was found to be **38**, which gave gold-coloured films of stoichiometric $TiN_{1.0}$. However, it was clear that the nitrogen content varied from stoichiometric using **38** ($TiN_{1.0}$) to non-stoichiometric when using, for example $[TiCl_2(N^iPr)(Me_3[6]aneN_3)]$ and $[TiCl_2(NPh)(NHMe_2)_2]$ ($TiN_{0.2}$). XRD showed the presence of titanium nitride and, in certain samples, anatase (TiO_2). The films that contained only TiN were produced by decomposition of **38** and also the compound $[TiCl_2(NC_6H_3Me_2\text{-}2,6)(NHMe_2)_2]$. An additional anatase phase was detected by XRD in the films derived from $[TiCl_2(N^iPr)(NHMe_2)_2]$ and $[TiCl_2(N^tBu)(Me_3[6]aneN_3)]$ and the rest of the compounds produced amorphous films. Therefore, despite the coordination environment around the metal being essentially the same and the compounds having comparable volatility, significant differences in film quality were observed. In this related series of compounds, the question arises as to what makes a good single-source precursor for TiN films? The best precursor for TiN in this study was found to be **38**, which is the simplest of these imido complexes, possessing good leaving groups, such as the ^{t}Bu group that could leave as isobutylene and also the pyridines are expected to be labile. Chlorine contamination of the films was not observed above detection limits (1 atom%) despite all of the precursors having two Ti—Cl bonds. Therefore, the chlorides are both readily lost during film formation although it is not clear what decomposition pathway the chlorine loss follows since no active hydrogen is present for the loss of HCl, however, the direct loss of Cl_2 is possible. Overall compound **38** appeared to be an improvement over the widely used $[Ti(NMe_2)_4]$.

A selection of tungsten imido compounds, including $[W(\mu\text{-}N^tBu)(N^tBu)Cl_2(H_2N^tBu)]_2$ (**39**), $[W(N^tBu)_2Cl_2(TMEDA)]$

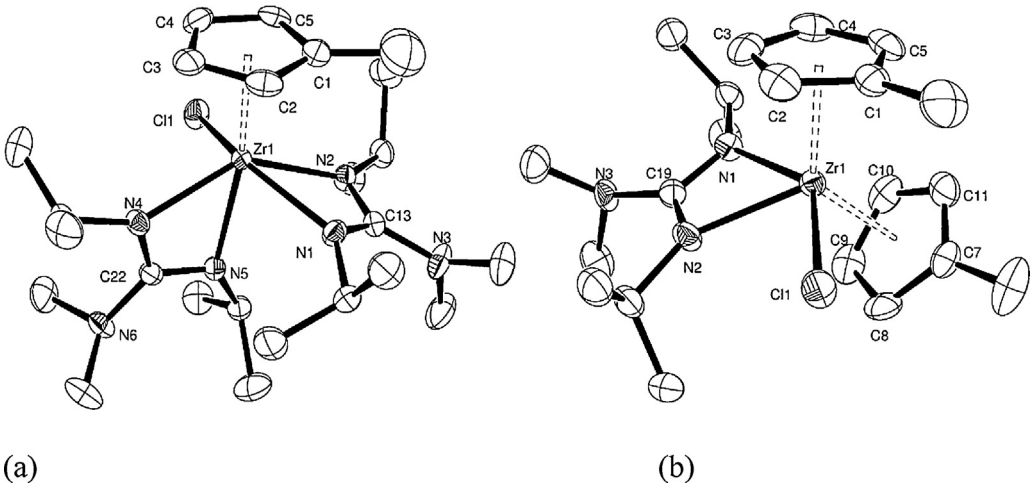

Fig. 18. ORTEP plot of (a) compound **36** and (b) compound **37** with 50% probability ellipsoids. H atoms omitted for clarity. Reprinted with permission from Ref. [88]. Copyright 2009 American Chemical Society.

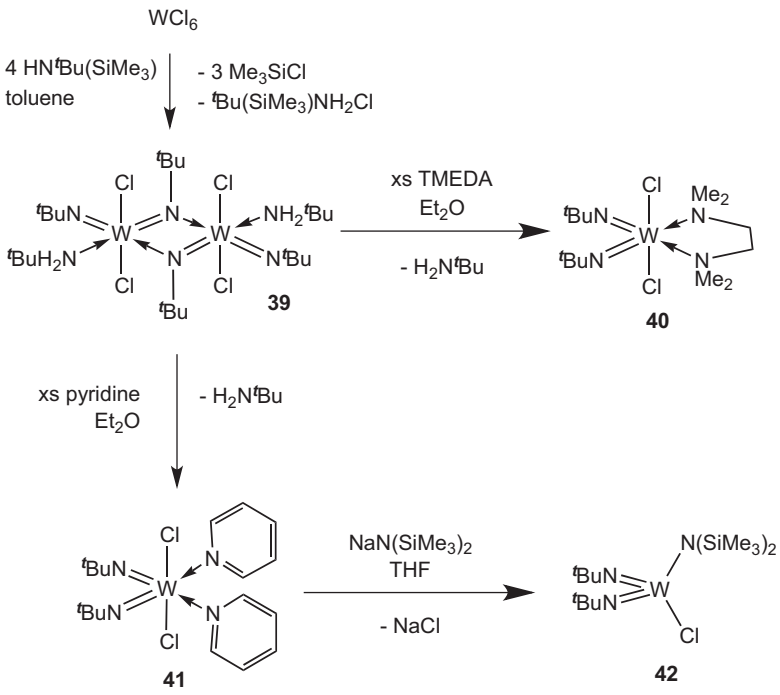

Scheme 12. Synthesis of compounds **39**–**42** [92–94].

(**40**), (TMEDA = *N*,*N*,*N*′,*N*′-tetramethylethylenediamine), $[W(N^tBu)_2Cl_2(py)_2]$ (**41**), (py = pyridine) and $[W(N^tBu)_2Cl\{N(SiMe_3)_2\}]$ (**42**), have been examined as potential LPCVD and AACVD precursors [92]. Compounds **30**–**41** were synthesized via modified literature procedures, as depicted in Scheme 12 [93,94]. However, compound **42** was synthesized from the reaction of **41** with one equivalent of $NaN(SiMe_3)_2$ (Scheme 12). A liquid precursor is preferable for CVD and **42** could only be isolated as an oil, however spectroscopic data (NMR and mass spectroscopy) provided evidence that the compound existed as a monomer.

The vapour pressures of **39**–**41** were determined to be greater than 1 mTorr at 50 °C and LPCVD of these compounds and **42** resulted in the deposition of grey mirror-like crystalline films of β-WN_xC_y. The films were adhesive, uniform, hard and abrasion resistant being resistant to scratching with a steel scalpel. In all cases the chlorine contamination of the films was minimal (less than 1 at%) and the films were deposited with either a nitrogen or ammonia bleed. The presence of ammonia reduced the oxygen content of the films, but surprisingly did not significantly change the carbon content of the resulting films. Where nitrogen was employed as the bleed gas, the films were generally nitrogen-rich as the W:N ratio varied over the range 1:1.12–1.35, with W:C ratios not exceeding 1:0.3 (Table 1). The exception was the film deposited from compound **40**, where the W:N ratio was less than 1 (W:N = 1:0.95). Also in this case, the W:C ratio was higher (W:C = 1:0.87). This is not unexpected as the TGA data showed a lower mass loss than expected, implying that the ligands in compound **40** will contribute significantly more to carbon contamination than the other compounds. Therefore, despite the coordination environment around the metal being similar and the compounds having comparable volatility, some differences in film quality were observed.

Table 1
Film compositions for the b-WN_xC_y films deposited via LPCVD from compounds **39–42** as determined by WDX [94].

Precursor	Composition from WDX	
	Nitrogen bleed	Ammonia bleed
39	$WN_{1.18}C_{0.22}$	$WN_{1.32}C_{0.23}$
40	$WN_{0.95}C_{0.87}$	$WN_{1.13}C_{0.27}$
41	$WN_{1.35}C_{0.29}$	$WN_{1.23}C_{0.20}$
42	$WN_{1.12}C_{0.20}$	$WN_{1.20}C_{0.24}$

AACVD of compound **39** resulted in the deposition of amorphous tungsten carbonitride films. WDX indicated that the compositions of the films were $WN_{0.41}C_{0.26}$ and there was considerable chlorine contamination. These results suggest that these compounds serve better as single-source precursors, or dual-source in the presence of ammonia, in a LPCVD technique rather than AACVD.

4.3. Titanium phosphine and arsine complexes

A range of complexes of the type $[TiCl_4(L)_2]$ (L = $PhPH_2$, Ph_2PH, PPh_3, $CyPH_2$, Cy_2PH (**43**), PCy_3) and $[TiCl_4(L')]$ (L′ = dppm, dppe (**44**) or dppp) have been synthesized, via the reaction of $TiCl_4$ with the relevant phosphine, as potential precursors to titanium phosphide thin films [95]. We were particularly interested in studying the effect of changing the phosphine ligand on the resulting film composition. Compounds **43** and **44** were structurally characterized and both complexes were found to exhibit a distorted octahedral coordination geometry where the phosphine ligands are *trans* in **43** but *cis* in **44** due to the presence of the chelating phosphine ligand (Fig. 19).

LPCVD of all of the compounds was investigated at 550 °C, which showed that $[TiCl_4(L)_2]$ (L = $CyPH_2$, Cy_2PH and PCy_3) and $[TiCl_4(dppm)]$ were effective titanium phosphide precursors, whereas $[TiCl_4(L)_2]$ (L = $PhPH_2$, Ph_2PH and PPh_3) and $[TiCl_4(dppp)]$ did not produce a film under the same conditions. Interestingly, $[TiCl_4(dppe)]$ produced a film containing only titanium (no P) under similar conditions. For the compounds which produced titanium phosphide films, almost stoichiometric TiP films were deposited from precursor **43** but the composition of the films deposited from the other compounds changed from $Ti_{1.1}P$ to Ti_3P.

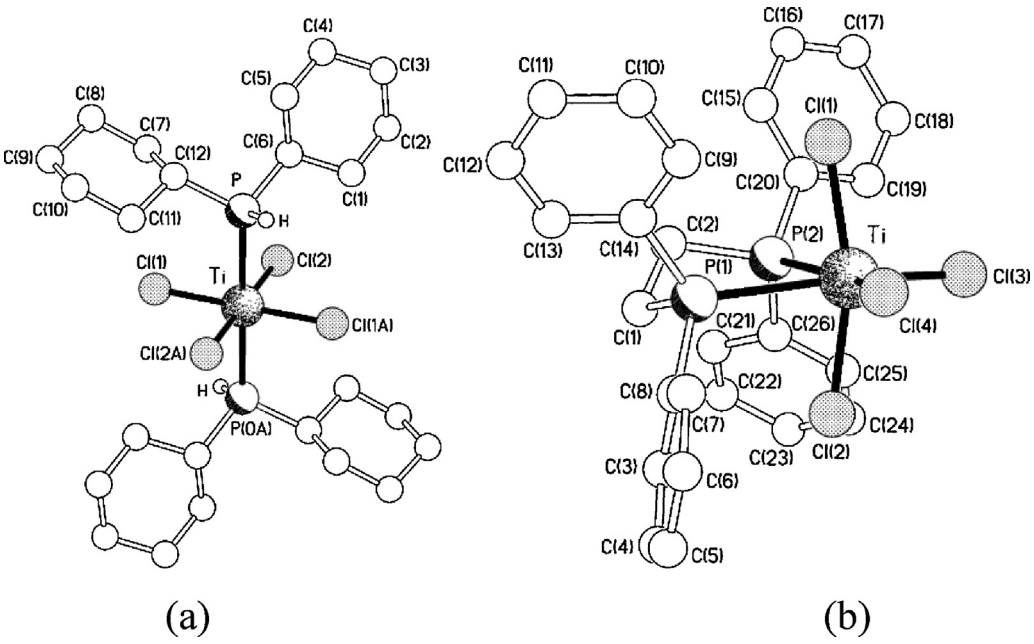

Fig. 19. Molecular structure of (a) compound **43** and (b) compound **44**. H atoms omitted for clarity.
Reprinted with permission from Ref. [95]. Copyright 2002 Royal Society of Chemistry.

All the films deposited were amorphous. Overall the differences observed in the films (or lack of films) produced from the different precursors indicated that complexes with primary or secondary phosphines ($CyPH_2$ and Cy_2PH) were superior titanium phosphide precursors.

Single-source precursors available for the deposition of transition metal arsenide thin films are limited and based on the successful deposition of TiP films from phosphine adducts of $TiCl_4$ some related arsine adducts were synthesized as potential precursors to TiAs. The single-source route to TiAs was investigated as it uses less toxic precursors (than for example AsH_3 employed in conventional dual-source CVD routes) and considerably less complicated apparatus. Therefore, arsine adducts of titanium(IV), of the type $[TiCl_4(L)_n]$ ($n = 1$, L = $AsPh_3$, $Ph_2AsCH_2AsPh_2$, and $^tBuAsH_2$; $n = 2$, L = $AsPh_3$) were isolated and investigated as precursors to TiAs [96]. However, the weak Ti—As donor bonds resulted in oxidation and formation of titanium oxide and the very air sensitive nature of the precursors resulted in problems with the single-source route and manipulation. In contrast, dual-source atmospheric pressure CVD of $TiCl_4$ and $^tBuAsH_2$ resulted in the formation of highly reflective titanium arsenide films, probably due to the presence of excess arsine in this method reducing oxidation of the films [97].

5. Conclusion

A range of precursors to gallium and indium oxide have been developed, based on donor-functionalized alkoxides, ketoiminates and diketonates. The nature and purity of the precursor used can affect the composition and structure of the resulting film since the key step in film deposition is the decomposition of the precursor. This was shown clearly from the use of the related compounds $[Me_2Ga(OR')]_2$ and $[Et_2Ga(OR')]_2$, where the methyl derivative resulted in carbon contamination whereas the ethyl groups have a more facile decomposition route, via β-hydride elimination, and no carbon contamination was observed. Ideally, ligands need to be cleanly lost during the decomposition process in the gas phase but should also provide stability to the starting precursor. The type of ligand is therefore very important but for each deposition technique different requirements are best met by different precursors, i.e. a compound that gives good film deposition under the conditions of one technique may not undergo deposition when used in an alternative deposition methodology. The donor-functionalized alkoxides have proved to be an excellent choice of ligand since GED studies indicated that the 'donor-arm' in the ligand stabilized monomeric species in the gas phase and hence enhanced volatility.

The main technique used in our studies for the deposition of high quality films of gallium and indium was aerosol-assisted CVD. In this deposition technique solubility is the key requirement for the precursor and the use of 'donor arms' in some of the ligands, such as the donor-functionalized alkoxides and ketoiminates, has resulted in highly soluble precursors that show good stability in solution. Many of the precursors have afforded highly transparent films with excellent coverage of the substrate. Some of the key applications of these films actually require the use of impurity-doped metal oxides, for example TCO materials such as Ga-doped ZnO and Ga-doped indium oxide. We have shown that AACVD is an excellent technique for the formation of doped-metal oxides with the formation of Ga-, Ta- and Ti-doped indium oxide films. AACVD also has the advantage that the precursor can be formed in situ in the CVD bubbler and this therefore removes the necessity to prepare, isolate and purify complicated precursors. This is an important point since precursors should be easily synthesized in high-yielding reactions to be suitable for scale-up in industrial processes.

Solution-based processes are ideal for coating flexible substrates and the development of soluble single-source precursors is crucial. Currently, TCOs are widely used for rigid devices but the technology used to coat rigid substrates is not always applicable for coating flexible substrates. As more flexible devices are required to incorporate into a range of applications, such as flexible displays for e-readers and OLEDs, flexible barrier layers such as TCOs will be in demand.

In the area of transition metal pnictides we have developed metal guanidinate complexes to improve thermal stability and

provide a nitrogen bound coordination sphere. For some precursors, carbonitride films rather than nitride were deposited, which shows that careful choice of the ligand is extremely important. We have also shown that titanium and tungsten imido compounds are excellent precursors but simple Lewis base adducts, such as phosphines and in particular arsines are not as suitable to serve as single-source precursors. We also observed that LPCVD is a far superior technique for the formation of metal pnictides and AACVD largely resulted in oxidation. Thus, the latter technique appears to be more useful for the formation of metal oxides.

Further refinement of precursor design for the CVD of both metal oxides and nitrides should lead to additional control over the composition of the material deposited, as well as determining the optimum deposition conditions, all of which are important for the various applications of these materials.

Acknowledgements

Much of the work described in this review was supported by EPSRC (EP/F035675, EP/C513649, GR/R16518, GR/M98630 and GR/M98623) and we are grateful for their continued support. We also thank our co-workers acknowledged in the various references and support from Pilkington NSG and SAFC Hitech.

References

[1] A.C. Jones, M.L. Hitchman, Chemical Vapour Deposition: Precursors, Processes and Applications, vol. 1199, Roy. Soc. Chem., 2008, Chapter 1, pp 1–36.
[2] L. Bloor, C.J. Carmalt, D. Pugh, Coord. Chem. Rev. 255 (2011) 1293.
[3] M.A. Malik, M. Afzaal, P. O'Brien, Chem. Rev. 110 (2010) 4417.
[4] X. Hou, K.-L. Choy, Chem. Vapor Depos. 12 (2006) 583.
[5] P. Marchand, I. Hassan, I.P. Pakin, C.J. carmalt, Dalton Trans., submitted for publication.
[6] C.J. Carmalt, S.J. King, Coord. Chem. Rev. 250 (2006) 682.
[7] M.G. Blamire, J.L. MacManus-Driscoll, N.D. Mathur, Z.H. Barber, Adv. Mater. 21 (2009) 3827.
[8] C.G. Granqvist, A. Hultåker, Thin Solid Films 411 (2002) 1.
[9] H.L. Hartnagel, A.L. Dawar, A.K. Jain, C. Jagadish, Semiconducting Transparent Thin Films, IOP Publishing, Bristol, 1995.
[10] T. Maruyama, K. Fukui, Jpn. J. Appl. Phys. 29 (1990) L1705.
[11] R. Nomura, K. Konishi, H. Matsuda, J. Electrochem. Soc. 138 (1991) 631.
[12] A.C. Wang, N.L. Edleman, J.R. Babcock, T.J. Marks, M.A. Lane, P.R. Brazis, C.R. Kannewurf, J. Mater. Res. 17 (2002) 3155.
[13] R. Street, Technology and Applications of Amorphous Silicon, Springer, New York, 2000.
[14] C.G. Granqvist, Sol. Energy Mater. Sol. Cells 91 (2007) 1529.
[15] F. Zhuge, L.P. Zhu, Z.Z. Ye, D.W. Ma, J.G. Lu, J.Y. Huang, F.Z. Wang, Z.G. Ji, S.B. Zhang, Appl. Phys. Lett. 87 (2005) 092103.
[16] J.G. Lu, Z.Z. Ye, F. Zhuge, Y.J. Zeng, B.H. Zhao, J.Y. Huang, Appl. Phys. Lett. 85 (2004) 3134.
[17] M. Fleischer, H. Meixner, Sens. Actuators B 13 (1993) 259.
[18] Z. Liu, T. Yamazaki, Y. Shen, T. Kikuta, N. Nakatani, Y. Li, Sens. Actuators B 129 (2008) 666.
[19] H.L. Ma, D.W. Fan, Chin. Phys. Lett. 26 (2009) 117302.
[20] M. Fleischer, H. Meixner, Sens. Actuators B 4 (1991) 437.
[21] J. Frank, A. Fleischer, A. Zimmer, H. Meixner, IEEE Sens. J. 1 (2001) 318.
[22] L.G. Bloor, J. Manzi, R. Binions, I.P. Parkin, D. Pugh, A. Afonja, C.S. Blackman, S. Sathasivam, C.J. Carmalt, Chem. Mater. 24 (2012) 2864.
[23] X. Lai, D. Wang, N. Han, J. Du, J. Li, C. Xing, Y. Chen, X. Li, Chem. Mater. 22 (2010) 3033.
[24] P. Meriaudeau, C. Naccache, J. Mol. Catal. 59 (1990) L31.
[25] S.C. Vanithakumari, K.K. Nanda, Adv. Mater. 21 (2009) 3581.
[26] S. Daniele, D. Tcheboukov, L.G.H. Pfalzgraf, J. Mater. Chem. 12 (2002) 2519.
[27] A.C. Taş, P.J. Majewski, F. Aldinger, J. Am. Ceram. Soc. 83 (2000) 2954.
[28] K.R. Reyes-Gil, E.A. Reyes-Garcia, D. Raftery, J. Phys. Chem. C 111 (2007) 14579.
[29] Y. Sakata, Y. Matsuda, T. Yanagida, K. Hirata, H. Imamura, K. Teramura, Catal. Lett. 125 (2008) 22.
[30] W.A. Hermann, N.W. Huber, O. Runte, Angew. Chem. Int. Ed. Engl. 34 (1995) 2187.
[31] L.G. Hubert-Pfalzgraf, Coord. Chem. Rev. 178 (1998) 967.
[32] C.E. Knapp, L. Pemberton, C.J. Carmalt, D. Pugh, P.F. McMillan, S.A. Barnett, D.A. Tocher, Main Group Chem. 9 (2010) 31.
[33] S. Basharat, C.J. Carmalt, R. Palgrave, S.A. Barnett, D.A. Tocher, H.O. Davies, J. Organomet. Chem. 693 (2008) 1787.
[34] S. Basharat, C.J. Carmalt, S.J. King, E.S. Peters, D.A. Tocher, Dalton Trans. (2004) 3475.
[35] S. Basharat, C.J. Carmalt, S.A. Barnett, D.A. Tocher, H.O. Davies, Inorg. Chem. 46 (2007) 9473.
[36] Z. Hajanal, J. Miro, G. Kiss, F. Reti, P. Deak, R.C. Herndon, J.M. Kuperberg, J. Appl. Phys. 86 (1999) 3792.
[37] M. Valet, D.M. Hoffman, Chem. Mater. 13 (2001) 2135.
[38] J. Tauc (Ed.), Proceedings of the International School of Physics, Enrico Fermi, Course XXXIV, 1966.
[39] J. Passlack, Appl. Phys. 77 (1995) 686.
[40] D. Vemardou, M.E. Pemble, D.W. Sheel, Thin Solid Films 515 (2007) 8768.
[41] C.E. Knapp, D.A. Wann, A. Bil, J.T. Schirlin, H.E. Robertson, P.F. McMillan, D.W.H. Rankin, C.J. Carmalt, Inorg. Chem. 51 (2012) 3324.
[42] C.E. Knapp, C.J. Carmalt, P.F. McMillan, D.A. Wann, H.E. Robertson, D.W.H. Rankin, Dalton Trans. (2008) 6880.
[43] S. Basharat, C.E. Knapp, C.J. Carmalt, S. Barnett, D.A. Tocher, New J. Chem. 32 (2008) 1513.
[44] C.E. Knapp, D. Pugh, P.F. McMillan, I.P. Parkin, C.J. Carmalt, Inorg. Chem. 50 (2011) 9491.
[45] S. Basharat, C.J. Carmalt, R. Binions, R. Palgrave, I.P. Parkin, Dalton Trans. (2008) 591.
[46] C.R. Pulham, A.J. Downs, M.J. Goode, D.W.K. Rankin, H.E. Robertson, J. Am. Chem. Soc. 113 (1991) 5149.
[47] D. Pugh, L.G. Bloor, I.P. Parkin, C.J. Carmalt, Chem. Eur. J. 18 (2012) 6079.
[48] A.W. Addison, T.N. Rao, J. Reedijk, J. van Rijn, G.C. Verschoor, J. Chem. Soc., Dalton Trans. (1984) 1349.
[49] M. Munoz-Hernandez, P. Wei, S. Liu, D.A. Atwood, Coord. Chem. Rev. 210 (2000) 1.
[50] S. Basharat, W. Betchley, C.J. Carmalt, S. Barnett, D.A. Tocher, H.O. Davies, Organometallics 26 (2007) 403.
[51] A. Ortiz, J.C. Alonso, E. Andrade, C. Urbiola, J. Electrochem. Soc. 148 (2001) F26.
[52] G.A. Battison, R. Gerbasi, M. Porchia, R. Bertoncello, F. Caccavale, Thin Solid Films 279 (1996) 115.
[53] G.E. Coates, R.G. Hayter, J. Chem. Soc. (1953) 2519.
[54] O.T. Beachley Jr., J.R. Gardinier, M.R. Churchill, L.M. Toomey, Organometallics 22 (2003) 1145.
[55] D. Pugh, P. Marchand, I.P. Parkin, C.J. Carmalt, Inorg. Chem. 51 (2012) 6385.
[56] A. Aprile, D.J. Wilson, A.F. Richards, Dalton Trans. 41 (2012) 8550.
[57] C.E. Knapp, G. Hyett, I.P. Parkin, C.J. Carmalt, Chem. Mater. 23 (2011) 1719.
[58] C.E. Knapp, A. Kafizas, I.P. Parkin, C.J. Carmalt, J. Mater. Chem. 21 (2011) 12644.
[59] A. Kafizas, C.W. Dunnill, I.P. Parkin, J. Mater. Chem. 20 (2010) 8336.
[60] B. Xia, Y.S. Chu, W.L. Gladfelter, Surf. Coat. Technol. 201 (2007) 9041.
[61] G. Korotcenkov, Mater. Sci. Eng. B (2007) 1.
[62] G.S. Devi, S.V. Manorama, V.J. Rao, Sens. Actuators B 56 (1999) 98.
[63] A.M. Azad, S. Larose, S.A. Akbar, J. Mater. Sci. 29 (1994) 4135.
[64] H. Heidong, Q. Wei, W. Xiaohong, D. Xianbo, C. Long, J. Zhaohua, Thin Solid Films 515 (2007) 5362.
[65] B.H. Park, B.S. Kang, S.D. Bu, T.W. Noh, J. Lee, W. Jo, Nature 401 (1999) 682.
[66] M.K. Singh, Y. Yang, C.G. Takoudis, Coord. Chem. Rev. 253 (2009) 2920.
[67] C. Michel, M. Hervieu, M.M. Borel, A. Grandin, F. Deslandes, J. Provost, B. Raveau, Z. Phys B: Condens. Matter 68 (1987) 421.
[68] L. Leontie, M. Caraman, M. Alexe, C. Harnagea, Surf. Sci. 507 (2002) 480.
[69] L. Zhang, W. Wang, J. Yang, Z. Chen, W. Zhang, L. Zhou, S. Liu, Appl. Catal. A 308 (2006) 105.
[70] L. Zhou, W. Wang, H. Xu, S. Sun, M. Shang, Chem. Eur. J. 15 (2009) 1776.
[71] K. Gurunathan, Int. J. Hydrogen Energy 29 (2004) 933.
[72] M. Mehring, Coord. Chem. Rev. 251 (2007) 974.
[73] S.J.A. Moniz, C.S. Blackman, C.J. Carmalt, G. Hyett, J. Mater. Chem. 20 (2010) 7881.
[74] P.A. Williams, A.C. Jones, M.J. Crosbie, P.J. Wright, J.F. Bickley, A. Steiner, H.O. Davies, T.J. Leedham, G.W. Critchlow, Chem. Vapor Depos. 7 (2001) 205.
[75] M.C. Massiani, R. Papiernik, L.G. Hubert-Pfalzgraf, J.-C. Daran, Polyhedron 10 (1991) 437.
[76] S.J.A. Moniz, D. Bhachu, C.S. Blackman, A.J. Cross, S. Elouali, D. Pugh, R.Q. Cabrera, S. Vallejos, Inorg. Chim. Acta 380 (2012) 328.
[77] A.J. Perry, M. Georgson, W.D. Sproul, Thin Solid Films 157 (1988) 255.
[78] D.M. Hoffman, R. Fix, R.G. Gordon, Chem. Mater. 2 (1990) 235.
[79] L. McElwee-White, O.J. Bchir, S.W. Johnston, A.C. Cuadra, T.J. Anderson, C.G. Ortiz, B.C. Brooks, D.H. Powell, J. Cryst. Growth 249 (2003) 262.
[80] L. McElwee-White, Dalton Trans. (2006) 5327.
[81] H.O. Pierson, Handbook of Refractory Carbides and Nitrides. 4: Carbides of Group IV, William Andrew Publishing, Norwich, NY, 1996, p. 55.
[82] R. Fischer, A. Devi, R. Bhakta, A. Milanov, M. Hellwig, D. Barreca, E. Tondello, R. Thomas, P. Ehrhart, M. Winter, Dalton Trans. (2007) 1671.
[83] B. Nolang, O. Eriksson, B. Johansson, J. Solid State Chem. 86 (1990) 300.
[84] K. Komaki, Japanese Patent JP 02 248 079, 1990.
[85] A. Kafizas, C.J. Carmalt. I.P. Parkin, Coord. Chem. Rev., http://dx.doi.org/10.1016/j.ccr.2012.12.004
[86] F.T. Edelmann, Adv. Organomet. Chem. 57 (2008) 183.
[87] C.J. Carmalt, A.C. Newport, S.A. O'Neill, I.P. Parkin, A.J.P. White, D.J. Williams, Inorg. Chem. 44 (2005) 615.
[88] S.E. Potts, C.J. Carmalt, C.S. Blackman, F. Abou-Chahine, D. Pugh, H.O. Davies, Organometallics 28 (2009) 1838.
[89] C.J. Carmalt, A. Newport, I.P. Parkin, P. Mountford, A.J. Sealey, S.R. Dubberley, J. Mater. Chem. 13 (2003) 84.
[90] C.J. Carmalt, A.C. Newport, I.P. Parkin, A.J.P. White, D.J. Williams, J. Chem. Soc., Dalton Trans. (2002) 4055.
[91] A.J. Blake, P.E. Collier, S.C. Dunn, W.S. Li, P. Mountford, O.V. Shishkin, J. Chem. Soc., Dalton Trans. (1997) 1549;

P.J. Wilson, A.J. Blake, P. Mountford, M. Schroder, J. Organomet. Chem. 600 (2000) 71;
N. Adams, A.R. Cowley, S.R. Dubberley, A.J. Sealey, M.E.G. Skinner, P. Mountford, Chem. Commun. 12 (2001) 2738.
[92] S.E. Potts, C.J. Carmalt, C.S. Blackman, T. Leese, H.O. Davies, Dalton Trans. (2008) 5730.
[93] R.G. Gordon, J.S. Becker, S. Suh, S. Wang, Chem. Mater. 15 (2003) 2969.
[94] R.A. Fischer, A. Baunemann, D. Rische, M. Winter, Inorg. Chem. 45 (2006) 269.
[95] C.S. Blackman, C.J. Carmalt, I.P. Parkin, L. Apostolico, K.C. Molloy, A.J.P. White, D.J. Williams, J. Chem. Soc., Dalton Trans. (2002) 2702.
[96] T. Thomas, D. Pugh, I.P. Parkin, C.J. Carmalt, Dalton Trans. 39 (2010) 5325.
[97] T. Thomas, C.S. Blackman, I.P. Parkin, C.J. Carmalt, Eur. J. Inorg. Chem. (2010) 5629.